BSJ

UIC Bioengineering Student Journal

Spring 2020 Volume X Issue 1

BSJ

University of Illinois at Chicago Bioengineering Student Journal

Spring 2020

Vol. X No.1

Contact:
bioejour@uic.edu
Phone: (312) 996-2335 fax: (312) 996-5921
UIC Bioengineering Student Journal
Richard and Loan Hill Department of Bioengineering, University of Illinois at Chicago, Science & Engineering Offices (SEO), Room 218 (M/C 063)
bioe.uic.edu

BSJ IS A UNIVERSITY OF ILLINOIS AT CHICAGO BIOENGINEERING STUDENT PUBLICATION

UIC Bioengineering Student Journal
Spring 2020
Volume X, No.1

Contents

Foreword

On behalf of the Department of Bioengineering, I am happy to present the second issue of the tenth volume of the UIC Bioengineering Student Journal. This journal continues to strive to provide both graduate and undergraduate students an opportunity to gain experience writing research articles for an academic publication. This is a great opportunity for students to take the knowledge and skills learned in their coursework and research and apply it to write a paper relevant to the field of bioengineering. Students who participate in this student-led journal go through a rigorous review process in which students receive multiple peer-reviews and go through several rounds of editing until receiving final approval from the editorial board. As a result, students can improve their technical writing skills as well as their intercommunication skills, which will benefit them in their future careers.

I would like to thank our Faculty Advisor, Dr. Magin for his continuous support in helping us organize and further develop the journal. Also, I would like to thank our Department Head Dr. Royston for continually supporting the journal's financial and logistical needs and allowing us to host release parties every year. Lastly, I would like to thank and congratulate the authors, reviewers, and editors who consistently put their best effort forward to contribute to the completion and success of both issues of this year's journal even in this unprecedented time.

Anupriya Mathews
Editor-In-Chief
Volume X, Issue 1

Editor-In-Chief
Volume X, Issue 2

THE CURRENT DETECTION METHODS OF OVARIAN CANCER IN RADIOLOGY

Ritu Shah
rshah209@uic.edu

Abstract

According to the American Cancer Society, ovarian cancer accounts for over 22,000 deaths per year in the United States of America, and over 125,000 worldwide, making it the most lethal gynecologic malignancy. The low cure percentage is predominantly due to late diagnosis and consequent tumor dissemination. There are two diagnostic challenges when an ovarian mass is detected. The initial challenge is the detection of ovarian malignancy and the second challenge is the evaluation of tumor dissemination. Because a majority of ovarian masses are non-neoplastic cysts, diagnostic studies that allow accurate diagnosis is important to avoid unnecessary surgical procedures. Hence it is important to detect and evaluate ovarian cancer accurately and efficiently. This paper will examine the anatomy of ovaries, the different types of ovarian cancers, the roles of various radiological methods currently used to detect ovarian cancer, and future perspectives on how Artificial Intelligence could speed up the process of detection.

Keywords: *Ovarian Cancer, Single-photon emission computed tomography (SPECT), Positron emission tomography (PET), Magnetic resonance imaging (MRI), Ultrasound, Artificial Intelligence*

1. Introduction

1.1 Ovary Anatomy and Function

Ovaries are a vital organ in the female reproductive system like balancing hormones and producing eggs. The ovary is composed of germ cells and somatic cells. The interactions dictate the formation of oocyte-containing follicles, development oocytes and somatic cells, ovulation, and formation of the corpus luteum which help women maintain pregnancy.

Many events in the adult ovary are controlled by two hormones, follicle-stimulating hormone (FSH) and luteinizing hormone (LH), secreted from the anterior pituitary gland under the control of pulses of gonadotropin-releasing hormone (GnRH) from the hypothalamus (Figure 1) [9]. These hormones play a role in the menstrual cycle, enhancing follicle growth, ovulation, and the formation of the corpus luteum.

The ovary has a key role in ensuring the timely release of fertilizable oocytes and the maintenance of luteal cell function, a necessity for pregnancy, by directing feedback mechanisms to the hypothalamus and pituitary gland in the brain (Figure 1).

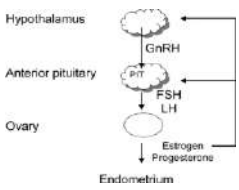

Figure 1. The role of the ovary in the reproductive system of women [2].

1.2 Ovarian Disorders

Ovarian cancer accounts for only 3 percent of cancers in women and is the fifth most common cause of cancer death in women [10]. In 2018, The American Cancer Society predicted there would be approximately 22,240 new cases of ovarian cancer diagnosed and 14,070 ovarian cancer deaths in the United States [10]. Ovarian cancer tends to develop from three kinds of tissue: approximately 85 to 95 percent from epithelial cells 5 to 8 percent from stromal cells, and 3 to 5 percent from germ cells [10]. These tissues begin from tumors that can be benign or malignant. Benign tumors cause very little harm compared to malignant tumors which are also called cancerous. Malignant tumors convert from benign once they have the capability to grow and spread to other organs forming cancerous structures or carcinomas. Epithelial, Stromal, and Germ cell are the various types of ovarian cancers.

1.3 Epithelial Ovarian Cancer

Epithelial cancer is most common in patients older than 50 years with at least 22,000 people who develop ovarian cancer worldwide [10]. 15 percent of epithelial cell ovarian cancers are borderline or have low malignant potential, with at least a 10-year survival period for 99 percent of patients who have had stage I ovarian cancer [10]. Epithelial ovarian cancers are further classified into Serous, Endometrioid, and Mucinous. Serous ovarian cancer contributes to 40 percent of all ovarian cancers [10]. Hence is the most

common classified ovarian cancer (Figure 2). Endometrioid ovarian cancer contributes to 20 percent of all ovarian cancers. Of which, 15 percent of endometrioid carcinomas coexist with endometriosis and 40 percent are bilateral, affecting both sides [10]. Mucinous ovarian cancer contributes to 25 percent of all ovarian cancers. This type of cancer can occur in association with endometriosis [10].

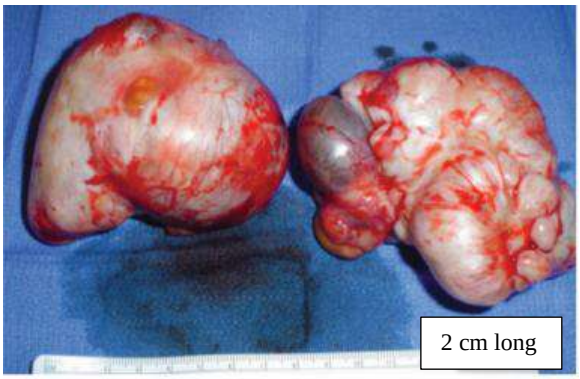

Figure 2. Serous epithelial ovarian tumors [10].

1.4 Stromal Ovarian Cancer

Stromal ovarian cancer contributes to 5 to 8 percent of all ovarian cancer types [10]. This type of cancer is derived from the sex cord of embryonic gonads. Granulosa-theca and Sertoli-Leydig are the further classifications of Stromal ovarian cancers. Granulosa-theca occurs in females of widespread age ranges and may produce precocious sexual development in prepubertal females. This type of cancer often can be associated with endometrial hyperplasia, cystic disease of the breast, and endometrial carcinoma in adults [10]. Sertoli-Leydig (Androblastomas) is common in adolescence, maybe masculinizing, which may block normal female sexual development [10].

1.5 Germ Cell Ovarian Cancer

Germ Cell Ovarian cancer contributes 3 to 5 percent of all ovarian cancer for children and adults between 20 – 30 years of age [10]. This type of cancer is highly malignant and usually unilateral, affects only one ovary. Germ cell ovarian cancer is further classified into Endodermal Sinus Tumor, Embryonal Extraembryonic, and Mature. Endodermal sinus tumor is the most common germ cell ovarian cancer in children and usually larger than 15 cm in diameter with the median age of patients being 18 years of age of which one-third of are premenarchal, before the onset of mensuration [10]. Embryonal (multipotential) Extraembryonic yolk sac carcinoma is much rare and is further classified into Primitive, Somatic, Trophoblast and Undifferentiated. Primitive is type of embryonal carcinoma is highly malignant and can cause precocious puberty. Undifferentiated carcinomas are the most common type of malignant germ cell ovarian cancer where, 10 to 20 percent are bilateral and radiosensitive [10]. Mature tumors are mostly benign cysts but can metastasis the ovaries and can further be referred to as Krukenberg tumors. 5 percent of these tumors can be served from breast or gastrointestinal sites and often turn malignant [10].

2. Traditional Detection Methods

2.1 Symptoms

Epithelial ovarian cancer is usually advanced quickly and tumor is often disseminated by the time it is diagnosed because the early stages of the disease have no obvious symptoms. The most common sign of the advanced disease is swelling of the abdomen caused by cysts. However, in some cases, women experience persistent, nonspecific symptoms in the months before diagnosis, including back pain, abdominal distension, pelvic or abdominal pain, difficulty eating or feeling full quickly, vomiting, indigestion, altered bowel habits, or urinary urgency or frequency. Women who have non-epithelial tumors, less common but significantly harder to diagnose, are often present with more specific early signs, including irregular vaginal bleeding. Additionally, sex cord-stromal tumors, such as Granulosa-theca and Sertoli-Leydig, often produce sex hormones that may affect menstruation and/or cause male physical characteristics, such as a deep voice or body hair which aid in the detection of advanced ovarian cancers. Although ovarian cancer is hard to detect, and most women find out much later since there are very few screening methods for detection [1].

2.2 Screening

Currently, there is no recommended screening test for ovarian cancer, although large-scale randomized clinical studies to identify effective screening modalities are an ongoing solution to the detection of ovarian cancer [1]. Ovarian cancer screening trial assesses ovarian cancer with the use of transvaginal ultrasound (TVU), sonography, and a fixed cut-point ($\geq$ 35 U/mL) in the tumor marker cancer antigen 125 (CA 125) for early detection [13]. Although these primary screening methods are available studies show low screening rates. The primary reasons for this are

- Debates whether screening of ovarian cancer is beneficial in early detection of ovarian cancer

- Screening for ovarian cancer in the general population without adequate evidence can often cause more harm than good, since surgical interventions in women without ovarian cancer is often required.
- Procedures for screening are often costly.
- A vast population often do not have access to these available options

Most women only get screening done after they experience severe symptoms. Once screening detects any suspicious lesions various imaging detection techniques are used to aid the diagnosis of ovarian cancers.

3. Imaging Techniques

Although, there are not many screening methods available in the detection of ovarian cancer there are various imaging techniques that are used to identify cancers after the onset of carcinomas. Some of these techniques are preferred based on specificity and sensitivity percentages. They are also preferred based on the invasiveness of the imaging technique and the cost. The most common of these imaging techniques are Ultrasound, Magnetic Resonance Imaging (MRI), Computed Tomography (CT), and Positron Emission Tomography (PET).

Table 1: This is a summary of various imaging techniques used in the detection of ovarian cancers based on specificity and sensitivity [10].

Type	Sensitivity (%)	Specificity (%)	Use
TVU	86	91	This technique is used after Transvaginal Ultrasound (TVU) for fine detection and characterization of adnexal masses.
MRI	91	88	Used of further delineation of indeterminate masses on TUS.
CT	90	75	Used for preoperative treatment and follow-ups.
PET	67	79	Used for evaluation of metastases, and detection of cancer antigens in known ovarian cancers, for example recurrences.

3.1 Ultrasound

Transvaginal Ultrasound (TVU) or Doppler Transvaginal Ultrasonography (DTU) are the first step detection method for women with ovarian cancers as an initial evaluation of adnexal masses. Adnexal mass is a growth that occurs in or near the uterus, ovaries, Fallopian tubes and connecting tissues [6]. Since it is easily accessible to women with abnormal symptoms during their physical examination but is non-ionizing. Non-ionizing medical imaging methods are usually preferred since they cause minimal harm to living tissues compared to ionizing imaging techniques which cause chemical changes in the body by breaking chemical bonds that can often lead to mutations in the genetic information of the cell. To image in the tissue Both TVU and DTU use probes with maximal frequencies ranging 2 to 8 MHz [8]. These probes send sound waves through the body that hit a boundary. Different tissues and bones let different amount of sound pass through. This difference in sound waves reflected, is picked up by the probe that is recorded by the machine.

Features suggestive of cancer in these techniques include complexity with solid and cystic areas, extramural fluid, echogenicity, wall thickening, septa, and papillary projections. Smooth-walled and sonolucent masses are usually benign. Malignant lesions may display an increased number and tortuosity of vessels on Doppler evaluation [1]. If TVU or DTU reveals suspicious properties, magnetic resonance imaging may be useful for further evaluation.

Figure 3 shows an image from TVU that is commonly used as a first step to detection of ovarian cancer. The next step is the measurement of metabolic activity that is performed using a doppler, in this case a DTU seen in Figure 4.

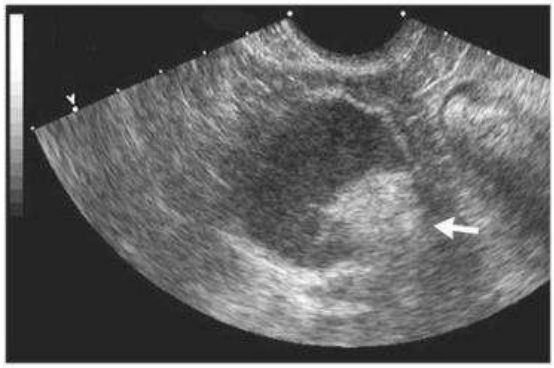

Figure 3. This is an image of a TVU mass in the right ovary shown with an arrow [1].

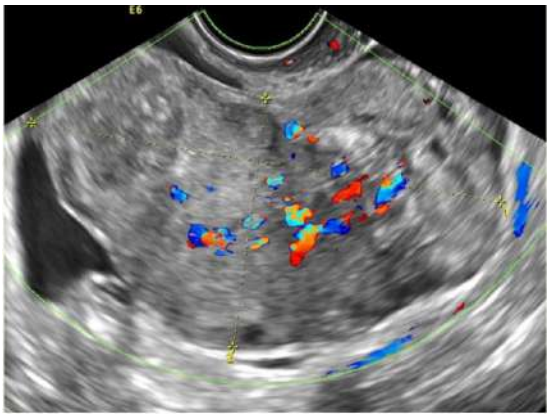

Figure 4. This is a DTU image of stromal cancer [6].

Although TVUs have a very high specificity of 91 percent and a sensitivity of 86 percent, they often are only used as a first measure (Table 1). Since other imaging modalities provide a larger field of view, have a shorter image acquisition time, and can be used while performing surgeries.

3.3 MRI

Magnetic resonance imaging (MRI), also known as nuclear magnetic resonance imaging (NMRI), is a scanning technique for creating detailed images of the human body. There are many forms of MRI, diffusion MRI, and functional MRI (fMRI) are two of the most common types. fMRI measures the metabolic function compared to MRI which just measure the anatomical structure.

In this technique the human body aligns to the magnetic field due to the hydrogen protons found in the human body in the form of water. An MRI scanner applies a very strong magnetic field of about 0.2 to 3 Teslas which aligns the proton spins [12]. This alignment (or magnetization) is next perturbed or disrupted by the introduction of an external Radio Frequency (RF) energy. The scanner also produces a radio frequency current that creates a varying magnetic field. The protons absorb the energy from the magnetic field and flip their spins. When the field is turned off, the protons gradually return to their normal spin, a process called precession. The return process produces a radio signal that can be measured by receivers in the scanner and made into an image. When the nuclei return to their resting alignment through various relaxation processes and in so doing emit RF energy. After a certain period following the initial RF, the emitted signals are measured.

Fourier transformation is used to convert the frequency information contained in the signal from each location in the image plane to corresponding intensity levels, which are then displayed as shades of gray in a matrix arrangement of pixels [12]. By varying the sequence of RF pulses applied and collected, different types of images are created. Repetition Time (TR) is the amount of time between successive pulse sequences applied to the same slice. Time to Echo (TE) is the time between the delivery of the RF pulse and the receipt of the echo signal. Tissue can be characterized by two different relaxation times – T1 and T2. T1 (longitudinal relaxation time) is the time constant which determines the rate at which excited protons return to equilibrium. This a measure of the time taken for spinning protons to realign with the external magnetic field. T2 (transverse relaxation time) is the time constant which determines the rate at which excited protons reach equilibrium or go out of phase with each other [12]. This also measures the time taken for spinning protons to lose phase coherence among the nuclei spinning perpendicular to the main field.

Women who clinically have a low risk of malignancy but have indeterminate lesions on ultrasound are the ones most likely to benefit from MRI. MRI is useful for definitively diagnosing many common benign adnexal lesions [4]. MRI is often helpful in visualizing the normal ovary and confirming the extraovarian nature of the lesion and better characterizes indeterminate adnexal lesions seen on ultrasound. A meta-analysis evaluating the incremental value of a second test for an indeterminate adnexal mass detected on gray-scale ultrasound determined that MRI with contrast administration or fMRI provided the highest posttest probability of ovarian cancer when compared with CT, Doppler ultrasound, or MRI without contrast administration [7]. MRI is a valuable in characterizing a complex cystic ovarian mass as an endometrioma and may detect signs of relatively rare malignant degeneration within it.

In Epithelial Ovarian Tumors MRI features of high-grade malignancies are predominantly cystic lesions with solid components, such as septate, mural nodules, and papillary projections. Cystic extraovarian lesions include peritoneal inclusion cysts, paratubal cysts, and hydrosalpinx [4]. The primary criteria for diagnosis of malignancy are large solid component, wall thickness, septal thickness and/or nodularity, and necrosis. Solid-appearing adnexal lesions include dermoids, exophytic uterine and broad ligament fibroids, and ovarian fibrothecoma.

Although most tumors can be identified, Borderline tumors are rarely diagnosed preoperatively because

they lack diagnostic imaging features that distinguish them from benign or early malignant epithelial tumors. On MRI, borderline tumors are predominantly cystic, with fluid ranging in T1 and T2 signal because of varying concentrations of protein and mucin. The diagnosis can be suggested based on these features in a younger patient with normal or only mildly elevated CA-125 levels [4]. MRIs typically help find cysts, mass, and tumors.

For example, Peritoneal inclusion cysts arise from pelvic adhesions that result from prior infections, surgery, or endometriosis. Fluid that is normally produced by the ovaries is trapped by the surrounding adhesions resulting in T1-hypointense and T2-hyperintense collections with thick or thin septations [4]. Hypo and Hyper refer to the shaded region of either T1 or T2 compared to other regions. Hypo meaning lighter and hyper meaning darker compared to other regions. Paratubal cysts are common developmental variants arising from duct remnants in the broad ligament [4]. On MRI, unilocular cysts are typically homogeneously T1-hypointense and T2-hyperintense lesions with no solid components. Fibroids, type of mass, can be low to high signal on T1- or T2-weighted images and hyper vascular to nonvascular on dynamic contrast-enhanced imaging [4]. The common MRI features of fibroids are that they are round, well-demarcated, displace rather than infiltrate surrounding structures, and often show homogeneous signal intensity and pattern of enhancement (Figure 5). Fibromas, thecomas, and fibrothecomas are solid benign ovarian tumors arising from sex cord and stromal cells. On MRI, their characteristic feature is internal homogeneity with low signal on both T1- and T2-weighted images. Fibrothecomas can sometimes be hormonally active, producing estrogen and causing malignancy [4].

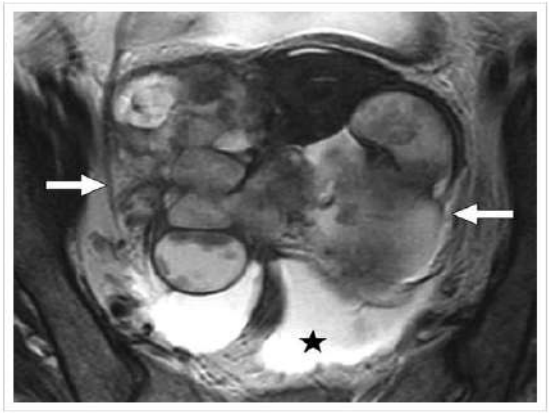

Figure 5. An MRI scan of a woman with Serous adenocarcinoma, the malignant masses are shown with arrows, the star represents ascites [4].

3.4 CT

A computerized tomography (CT) scan combines a series of X-ray images taken from different angles around your body and uses computer processing to create cross-sectional images, called slices, of the bones, blood vessels and soft tissues inside your body. CT scan images provide more-detailed information than plain X-rays do [12]. The downside to CT scans is the use of ionizing radiation and the amount of radiation is greater than you would get during a plain X-ray because the CT scan gathers more-detailed information. The low doses of radiation used in CT scans have not been shown to cause long-term harm, although at much higher doses, there may be a small increase in your potential risk of cancer. Hence, they have become a favored method for follow ups and pre-operative procedures.

CT is often the technique with which correct stages of ovarian cancer is detected because presenting symptoms of ovarian cancer indicates advanced disease and are typically nonspecific like abdominal pain or distention, urinary frequency, and early satiety [5]. Like shown in Figure. 6, CT is obtained to evaluate for intra-abdominal malignancy or ascites. Advanced ovarian cancer on CT typically presents as cysts with thick walls, septations, and papillary projections that are more clearly seen after contrast administration.

Although this pattern of disease is typical for ovarian cancer, other cancers like colon, gastric, and pancreatic cancers that ovarian metastases also can present similarly. Because ovarian cancer is treated with surgical cytoreduction often the radiologist tries to distinguish ovarian cancer from other tumors that may have similar presentations but require nonsurgical treatment [4]. Cytoreduction is when tumors are surgically removed before any other treatment like chemotherapy is performed. CT is also the preferred technique in the pretreatment evaluation of ovarian cancer to define the extent of disease and assess the likelihood of optimal surgical cytoreduction.

Although CT has many advantages like high specificity of 90 percent and 3-D view of images with more details it is only prescribed when other imaging methods have been tried since it is ionizing and has low sensitivity of 75 percent (Table 1). This can often cause more damage or predict the wrong stages of cancer depending on how much cytoreduction is done.

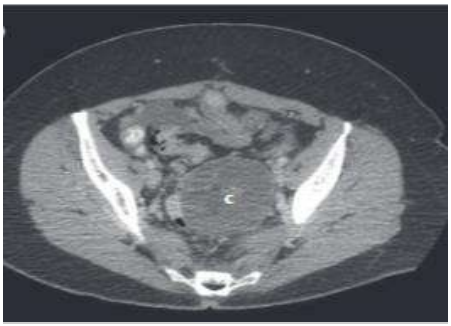

Figure 6. Common finding of an ovarian cancer mass on a CT scan denoted by the letter 'C' [5].

3.5 PET Nuclear Medicine

Positron emission tomography (PET) is a type of nuclear medicine procedure that measures metabolic activity of the cells of body tissues. PET is a combination of nuclear medicine and biochemical analysis. Used mostly in patients with brain or heart conditions and cancer, PET helps to visualize the biochemical changes taking place in the body, such as the metabolism. Metabolism is the process by which cells change food into energy after food is digested and absorbed into the blood. Specifically, PET studies evaluate the metabolism of a particular organ or tissue, so that information about the physiology such as functionality, and anatomy or structure of the organ or tissue that is evaluated, as well as its biochemical properties. Thus, PET may detect biochemical changes in an organ or tissue that can identify the onset of a disease process before anatomical changes related to the disease can be seen with other imaging processes such as CT or MRI. PET scans are also often a preferred method for cancer detection since carcinomas have a high metabolism. PET scans also provide a better advantage over other detection methods since they can identify tumor spreading in various parts of the body. PET differs from other nuclear medicine examinations in that PET detects metabolism within body tissues, whereas other types of nuclear medicine examinations detect the amount of a radioactive substance collected in body tissue in a certain location to examine the tissue's function.

PET is a type of nuclear medicine procedure, where a small amount of a radioactive substance like radioactive tracers are used during the procedure to assist in the examination of the tissue that is being examined (Figure 7). PET scans have a sensitivity 67 percent and a specificity of 79 percent, which is why it is not recommended for primary detection of ovarian cancer (Table 1). False-negative results have been reported with borderline tumors and low-grade and early carcinomas and false-positive results have also been reported with fibroids, and endometriosis [4]. The other downside of PET scans is it must be different for each woman based on their menstruation stage which includes premenopausal and post-menopausal stage. Since the activity of the ovaries is different for both. Although PET scans are good for various reasons, they are not preferred by themselves instead the combination of PET/CT is preferred since it covers specificity, sensitivity, and can be used for recurrences.

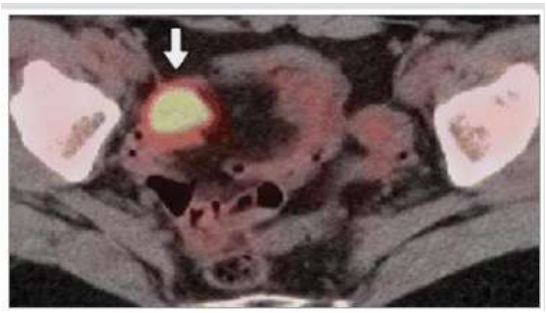

Figure 7. A PET scan of an ovarian lesion represented by an arrow [4]. The cancerous mass has a greater metabolic activity creating a bright spot on the PET scan.

3.6 PET/CT

Although not a preferred technique for cancer detection, a combination of PET/CT is playing an expanding role in treatment planning and follow-up. For predicting the correct stage, the addition of PET to contrast-enhanced CT has been shown to improve accuracy [7]. PET combined with CT, is the most accurate technique to evaluate for suspected recurrent ovarian cancer. A meta-analysis comparing techniques for detection of recurrence determined that PET/CT with sensitivity of up to 95 percent and a specificity of up to 90 percent. Which performed better than CT with sensitivity of 90 percent and a specificity of 75 percent or MRI with sensitivity of 91 percent and a specificity of 88 percent [10]. In addition, with fusion PET/CT, the CT images provide high-resolution, measurable information on the extent of disease and anatomic sites of involvement for treatment planning and follow-up.

4. Future Impact and Artificial Intelligence

Although, Artificial Intelligence (AI) is not widely used in cancer detection. Artificial intelligence techniques show a promising approach in detecting cancers using deep learning mechanisms where multiple collected images are stored in a network that can help identify future detection of cancer [3,11]. The application of AI would increase the rate of early

detection, reduce cost, and make the general detection of cancers a more efficient process.

5. Conclusion

A combination of PET/CT has shown promising results in detecting ovarian cancer. In addition, the use of artificial intelligence can make the process of detecting ovarian cancer much more efficient. The low survival percentage, of 47 percent for five years reported by the American Cancer Society, is predominantly due to late diagnosis and consequent tumor dissemination. As discussed, the two challenges of ovarian cancer are the process of detection and the evaluation of tumor dissemination. For future directions, the first step to overcoming this challenge can be facilitating more, accessible, and regular screening in women using ultrasound imaging systems. The second step is initiating a more standardized imaging procedure for women with ovarian cancer. Providing more accurate and sensitive imaging techniques like PET/CT can reduce the time frame of detection and metastasis to other organs of the body. Another essential step is incorporating AI in techniques like PET/CT scans that already show a potential in diagnosing ovarian cancer. In summary, improving procedures of detecting ovarian cancer could potentially benefit the detection of other cancers.

8. References

1. Clarke-Pearson, D. L. Screening for Ovarian Cancer. *The New England Journal of Medicine*. 361: 170 -177, 2009.

2. Hawkins, S. M., and M. M. Matzuk. The Menstrual Cycle. *Annals of the New York Academy of Sciences* .1135:10–18, 2008.

3. Hosny, A., C. Parmar, J. Quackenbush, L. H. Schwartz, and H. J. W. L. Aerts. Artificial intelligence in radiology. *Nature Reviews Cancer*. 18:500–510, 2018.

4. Iyer, V. R., and S. I. Lee. MRI, CT, and PET/CT for Ovarian Cancer Detection and Adnexal Lesion Characterization. *American Journal of Roentgenology*. 194:311–321, 2010.

5. Jayson, G. C., E. C. Kohn, H. C. Kitchener, and J. A. Ledermann. Ovarian cancer. *The Lancet.* 384:1376–1388, 2014.

6. Kamal, R., S. Hamed, S. Mansour, Y. Mounir, and S. A. Sallam. Ovarian cancer screening—ultrasound; impact on ovarian cancer mortality. *The British Journal of Radiology*. 91:20170571, 2018.

7. Kim, C. K., B. K. Park, J. Y. Choi, B.-G. Kim, and H. Han. Detection of Recurrent Ovarian Cancer at MRI. *Journal of Computer Assisted Tomography*. 31:868–875, 2007.

8. Nam, E. J., M. J. Yun, Y. T. Oh, J. W. Kim, J. H. Kim, S. Kim, Y. W. Jung, S. W. Kim, and Y. T. Kim. Diagnosis and staging of primary ovarian cancer: Correlation between PET/CT, Doppler US, and CT or MRI. *Gynecologic Oncology* 116:389–394, 2010.

9. Richards, J. S., and S. A. Pangas. The ovary: basic biology and clinical implications. *The Journal of Clinical Investigation*. 120: 963-972, 2010.

10. Roett, M. A., and P. Evans. Ovarian Cancer: An Overview. *American Family Physician*. 80:609-616, 2009.

11. Shimizu, A., K. Sawada, and T. Kimura. Development of novel approaches to detect ovarian cancer recurrence. *Journal of Medical Artificial Intelligence*.2:3–3, 2019.

12. Smith, N. B., and A. G. Webb. Introduction to medical imaging: physics, engineering, and clinical applications. Cambridge: Cambridge University Press, 2012.

13. Torre, L. A., B. Trabert, C. E. DeSantis, K. D. Miller, G. Samimi, C. D. Runowicz, M. M. Gaudet, A. Jemal, and R. L. Siegel. Ovarian cancer statistics. *Cancer Journal for Clinicians*. 68:284-296, 2018.

IDENTIFYING IMAGING TECHNIQUES THAT WILL BE ESSENTIAL FOR EARLY DIAGNOSIS OF IMPLANT COMPLICATIONS

Sandra Rivas
srivas3@uic.edu

Abstract

In 2010, 7.2 million individuals underwent orthopedic implant surgeries to receive a total knee replacement or total hip replacement. Orthopedic implants specialized in joint reconstruction account for 40 percent of orthopedic devices out in the market today. Although these devices are meant to last through the patient's lifetime, many complications may arise from metal debris within the body that cause inflammation and immune compromise. When a complication arises, the doctor may be hesitant to replace the implant because a lot of complications may arise from a revision surgery. Knowing exactly what is going on with the implant, or the biological interaction with the implant, is crucial. Before a revision surgery may be done, the doctor will have to ensure that the patient will need to undergo the surgery. The doctor will have to determine whether the surgery is needed depending on the patients age, active level, bloodwork, pain, and wear of the implant. This paper will focus on different medical imaging applications that can be used as a key contribution in early detection of complications arising from joint implants. These techniques will include the use of X-ray, ultrasound, CT, and MRI. It was concluded that surgeons should keep X-rays as the primary imaging technique to diagnose infections associated with orthopedic implants. Its ability to view detachment between implant and the bone and its inexpensive cost makes X-rays suitable for routine checks for implant related infection.

Keywords: *Medical Imaging, Orthopedic, Implants, X-ray, Ultrasound, MRI, CT*

1.Introduction

1.1 History of Orthopedic Implants

The birth of orthopedic implants is unclear. However, two of the key contributors in this medical field include Sir William Arbuthnot Lane and Albin Lambotte [3,16]. Prior to Lane and Lambotte, there are claims of surgeons using wire structure and ivory pegs to heal fractures. Lane and Lambotte used a combination of vanadium-iron for their implants. The idea was to choose a material that was durable. It was not until years later that surgeons began incorporating materials that were not only durable, but also biocompatible. The implants created by Lane and Lambotte were to be in vitro as the wound healed. Once the wound showed noticeable improvement, the implant was to be removed. The first recorded implant resembling present-day orthopedic implants was done by Ernest William Hey Grooves, which is shown in Figure 1 [23]. Records show that a peg composed of ivory was positioned in the hip to replace the head of the femur. This new form of implants became more accepted as new biomaterials were created alongside the discovery of antibiotics. In the 1990's the use of polylactic acid (PLA) and polyglycolic acid (PGA) began to be used in implants. This new material would eventually be absorbed by the body, as a result of this there was no need for a follow-up surgery to retrieve the implant. However, doctors found that some of these implants were rejected by the patient, leading to discomfort and sometimes pain.

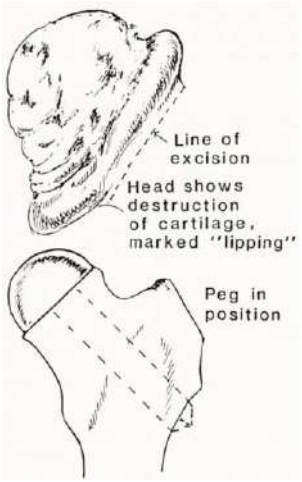

Figure 1. The image represents the first implant that resembles present-day permanent implants [23].

1.2 Different Types of Orthopedic Implants

Although there are numerous kinds of orthopedic implants, the most popular kind of implants concern the knees and hips. According to Mayo Clinic, 7.2 million patients in America have undergone surgery to receive a total knee replacement (TKR) or total hip replacement

(THR) [7]. TKR and THR are shown in Figure 2 and 3 respectively.

Figure 2. A representation of a TKR being used to replace a worn-out knee [9].

As people age, it is natural for their muscles, joints, and bones to wear down. There is a loss of bone density, calcium, and other minerals that consequently result in bones to become thinner. As the bones become thinner, they become more prone to pain or damage. Furthermore, the thinning of muscles and bones located in joints may reduce stability in patients, leading to instability when walking, which can cause falls. Falls in patients over 60 occur 49% of the time while walking, with half of these falls sustaining an injury [8]. This can explain why most of the TKR and THR surgeries required are for patients above 60. It was also cited that women are more likely to receive THR and TKR implants than men [7]. This can be due to menopause and pregnancies since both events can reduce the amount of calcium in women's bodies [19,1]. As a result, bones in women may be more fragile than men, and more likely to break.

Figure 3. A representation of a THR being done to replace a worn-down knee joint [18].

1.3 Different Complications That Arise from Implants.

Getting an implant is a big decision for patients. The surgery takes a big toll on the body, and since the majority of the patients receiving TKR and THR surgeries are over the age of 60, it is crucial to decide whether the surgery is needed. If the patient has chronic pain and movement problems in either the knees or the hip, and this pain is getting in the way of their everyday life, an orthopedic implant may be suggested [11]. Figure 4 shows inflammation that arises from a TKR. In this image, the inflammation caused by the infection is clearly seen, but in other cases this may not be true. Implants are said to last between 10-20 years; for many older patients this may last their whole lives. Although TKR and THR are said to be one of the most successful surgical procedures of all time, there are a percentage of patients that will need to undergo a revision surgery.

Table 1. Patient Demographics from [2], show the age and sex of patients that received revision surgery. Reprinted with permission from Clinical Orthopedics and Related Research.

Factor	Revision TKR people (%)	Revision THR people (%)
Age(years)		
<45	2430 (4)	13,877 (6)
45-54	9821 (15)	31,274 (13)
55-64	19,966 (30)	48,680 (21)
65-74	20,049 (30)	58,449 (25)
75-84	12,728 (19)	61,795 (26)
84+	2,540 (4)	21,781 (9)
Sex		
Men	28,233 (42)	100,053 (42)
Women	39,301 (58)	135,804 (58)

Revision surgery may arise from implant wear, loosening, dislocation, or fracture of implant. This paper focuses such as X-ray, ultrasound, CT, and MRI that can be used as a key contribution of complications arising from joint implants. 25% of reported failed TKR and 15% THA are due to infections. The statistics representing the age demographics relating to revision surgeries are displayed in Table 1.

2.Infections in the Body

According to Meital Zilberman, “An infection is a homeostatic imbalance between the host tissue and the presence of microorganisms” [25]. Depending on the extent of the infection, different actions may need to be taken. The infection may only require more antibiotics to be prescribed. Infections causing discomfort or pain may cause a revision surgery, and in extreme cases an amputation may be required. Infections can arise from contamination in the operating room, surgical equipment, or bacteria that is already present in the patient's body prior to surgery [22]. Infection that is caused by implants generally occur in two steps. The first step is that the bacteria attaches to the implant, leading to the second step, which is when biofilm is created where the implant is located [25]. The biofilm formed around the implant causes major problems. Biofilm is composed of exopolysaccharide, which is a type of bacteria that is highly dangerous due to its high resistance to antibiotics. This eliminates the possibility of using antibiotic therapy. The infection caused by the biofilm, if left untreated, can cause a chronic infection to occur. Thus, there are other methods of removing the infection that will have to be considered. In cases where the infection cannot be cured, the possibility of a revision surgery will have to be considered to remove the infected implant.

Figure 4. Inflammation caused by infection in a total knee replacement. [9].

3.Revision Surgery

3.1 Steps Prior to Revision Surgery

Deciding on whether a revision surgery is needed may be more complicated than receiving a TKR or THR surgery. As stated, the majority of the patients receiving these types of surgeries are over the age of 60, and another surgery might not be possible for them since complications increase with an increase of age. It has been shown that infections are one of the main causes of death in surgery in elderly patients [14]. It has also been found that revision surgeries might have a higher risk of surgical site infections [21]. The benefits of the surgery must outweigh the possible complications that may arise from performing the revision surgery. As a result, surgeons may ask for Erythrocyte sedimentation rate (EST) and C-reactive protein (CRP) blood work to be done on the patient [20]. EST is a test used to measure how much inflammatory activity is present in the body. CRP is a test that is used to measure c-reactive proteins in your bloodstream. This protein, synthesized by the liver, is delivered to the body when inflammation is present.

3.2 Medical Imaging for Early Detection

Two blood exams are used to identify whether an infection is present. The blood work can determine if the implant has caused any debris to spread throughout the body. Having a second form to verify the need and urgency of a revision surgery due to infection would be vital in early detection of complications in orthopaedic implants. It is vital to find research that is noninvasive which will decrease the risk of false positives and increase early detection of infections. Surgeons may be hesitant to perform surgery even if they see complications. It was stated that the doctor may not perform surgery until there is limited mobility or the infection of the implant is causing unbearable pain[20]. Therefore, abnormalities in soft tissue and bone are observed to see if the implant has caused any implant related infection. X-rays have been the primary use of medical imaging to observe implant failure. Doctors typically used X-rays to detect implant detachment or any degeneration of the bone. If there are any signs of a possible infection, doctors may need to confirm using fine needle aspiration. X-rays are not the only medical imaging technique that doctors use. There are several other techniques, however, each technique has its disadvantages. Table 2 is a comparison of the disadvantages that will be discussed in different imaging techniques to aid in correctly identifying an infection

Table 2. Disadvantages seen in Different Imaging Techniques [12]

Disadvantage	X-Ray	Ultrasound	Computerized Axial Tomography Scan (CT)	Magnetic Resonance Imaging (MRI)
Experience Beam Artifact	**X**		**X**	**X**
Unable to Image Bone		**X**		
Unable to Image Soft Tissue	**X**			
Expensive			**X**	**X**
Unable to Detect Blood Flow	**X**	**X**		
< 50% Sensitivity	**X**			
<50% Specificity	**X**			

4.Different Factors Concerning Early Detection of Orthopedic Related Infections

4.1 Beam Artifact

Beam artifact occurs in X-Ray, CT, and MRI imaging. This phenomenon is present due to the metal material present in orthopedic implants. In CT, the beaming artifact creates a high-pass filter to the X-ray beams, causing a distorted image. The distortion caused by the beam hardening artifact will vary depending on the composition of the implant. The distortion can be seen in Figure 5. The CT image is blurred compared to the X-ray image next to it.

Figure 5. The image is of a total hip replacement of the same patient. The picture on the left is an X-ray. The image on the right is using a CT imaging [4].

Beam hardening artifacts causes a distortion in the images taken; the image may show a difference in intensity at the center than at the edges. In reality, the material may be the same throughout. Beam hardening may also show up as streak discoloration in the image taken.

Factors that could affect the strength of beam artifacts present in the image include the materials used, the alignment of the implant to the magnetic field, complex shape or number of hardware parts, and the magnetic field strength [13,12]. It has been found that implants containing chromium-cobalt and stainless steel have worse beam hardening than implants with titanium. This is shown in Figure 6 [17,12]. Although beam hardening has been a big problem in imaging, new research has discovered ways to drastically reduce beam hardening to make these imaging techniques more useful in imaging metal objects, such as orthopedic implants.

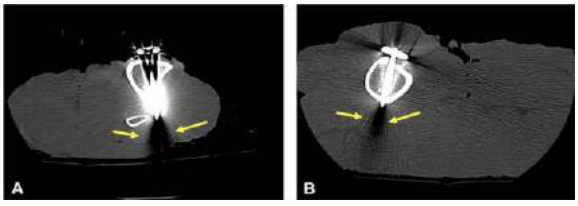

Figure 6. Figure A represents stainless steel and Figure B is titanium. Although both images observe beam hardening, it can be seen that A has a stronger beam hardening than B. These images were created by a CT scan [12]

As stated, MRIs have a high possibility of being distorted due to the prosthetic material surrounding the infected rejoin. MRIs are sensitive to specific tissue and tissue composure. Since prosthetic material can be found surrounding this type of tissue, the image generated from this MRI will not be a full representation of any possible infection [4].

4.2 Bone Imaging

Depending on the type of information a doctor is trying to obtain, the preferable imaging method may vary. Ultrasound is more ideal to read through soft tissue, but it would be ineffective in identifying any properties of the bone. An ultrasound of a THR is shown in Figure 7, where the doctors can identify periprosthetic fluid, a common property typically found near infections [17].

Figure 7. Ultrasound near a THR. A diagnosis cannot be determined because of the unclear image surrounding the area of interest. [17]

Being able to look at the bone to identify any deterioration or detachment to the implant would be beneficial in identifying if there is a problem. Detachment is known to occur if there is an infection present. Figure 8 and 9 are both X-rays exhibiting infection around the implants. In Figure 8, the infection is represented by the intra-articular gas. In Figure 8 the infection is identified by the darker color near the implants as opposed to seeing a light color that represents the bone, this verifies that the implant is not completely attached. Figure 9 shows an infected TKR that is loose. The looseness is identified by the lucency being shown in the white arrow. This is where the cement has detached from the bone. The open black arrow shows open space between the implant and the bone. The curved arrow represents the movement of the implant, since its implantation.

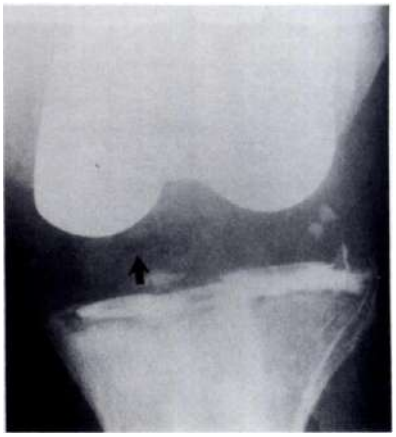

Figure 8. An X-ray of an infected total knee replacement is shown [21]. The dark arrow is pointing to untypical gas build up, which can be a sign of infection.

Figure 9. An X-ray of an infected TKR is shown [21]. The white and black hollow arrow represent detachments of the bone and the implant, and the curved arrow represents visible migration.

4.3 Soft Tissue Imaging

Soft tissue imaging is vital in observing infections in the body. Being able to observe abnormalities in soft tissue caused by infections would be an eminent technique in early detection of implant complications. Ultrasound is known to be able to be useful in analyzing soft tissue. On the contrary, an insufficient

amount of information will be recorded from areas such as the hip, due to its placement.

4.4 Cost of Imaging

Medical imaging is a business that raked over 100 billion in 2006[15]. Keeping a low cost on any medical procedure is essential to keep it obtainable to the majority of the population, and to make it ideal to be repeated. Imaging may be covered by most insurance plans, but a deductible may still be needed from the patient. As shown in Table 3 the most expensive type of medical imaging technique is MRI, where the most inexpensive is X-ray. This cost difference can also be reasoned due to the time needed to obtain an X-ray versus an MRI, which could take up to an hour to perform [10].

Table 3. Comparison Cost of Different Imaging Techniques [4].

Imaging Method	Fee for test	Fee for interpreting test	Total fee
MRI	$995	$123	$1,118
CT	$189	$44	$233
Ultrasound	$69	$20	$90
X-ray	$19	$9	$28

4.5 Blood Flow Detection

MRI machines are highly sensitive to flow phenomena. This means that MRIs can see the flow of fluids flowing throughout the body. If there were to be an infection caused by a prosthetic, there would be a large concentration of white blood cells flowing to the infected region. An MRI can detect this flow and indicate if there is an infection caused by a prosthetic. This detection can determine if a patient will have to undergo a revision surgery. Regular ultrasound cannot image blood flow. However, using ultrasound in doppler sonograms can be used to estimate the blood flow surrounding the implant [24]. This phenomenon cannot be detected by X-ray imaging. In conclusion, MRIs and doppler sonograms are best used for blood flow detection, unlike X-rays, where these are used more for solid bone structures.

4.6 Sensitivity and Specificity

22 patients with confirmed infections had CT images taken to identify if any infection in soft tissue could be identified, as well as to investigate if any fluid collection had occurred. It was concluded that there was 100% sensitivity and 87% specificity in true positive infections using CT imaging to identify infection in soft tissue. In comparison, there was a 100% specificity, but 16% sensitivity when identifying inflammation outside of the bone. Lastly, it has been concluded that 50% of radiographs show normal tissue, even though an infection may be present [2]. Although CT and MRI can aid in the detection of an infection, they are said to not be very useful in the early stages of infection where tissue damage is not as obvious [20].

5.Conclusion

After weighing in all the factors expressed in Table 1 it can be concluded that surgeons should keep X-rays as the primary imaging technique used for infections associated with orthopedic implants. The imaging technique that would be the worst would be the use of MRI. This can be concluded by the cost, beam artifact, and lack of bone imaging. X-ray are inexpensive, but they lack in detection of blood flow, beam artifact, and sensitivity, which are key contributors in identifying an infection. Since doctors are looking for early detection, being able to image bone and areas around the bone is crucial in identifying implant related infections. CT continues to improve its algorithms to remove beam hardening, but it is still relatively expensive and lacks bone imaging. Lastly, ultrasound was not able to record much data due to the area around the bone being the place of interest.

6.References

1. Aging changes in the bones - muscles - joints. at <https://medlineplus.gov/ency/article/004015.htm>. Accessed December 4, 2019.

2. Bozic, K. J., Kamath A. F., K. Ong, E. Lau, S. Kurtz, V. Chan, T. P. Vail, H. Rubash, and D. J. Berry. Comparative Epidemiology of Revision Arthroplasty: Failed THA Poses Greater Clinical and Economic Burdens Than Failed TKA. *Clinical Orthopaedics and Related Research.* 473:2131–2138, 2014.

3. Brand, R. A. Writing for Clinical Orthopedics and Related Research. *Clin. Orthopadeics and Related Research*. 413:1–7, 2009.

4. Cyteval, C., and A. Bourdon. Imaging orthopedic implant infections. *Diagnostic and Interventional Imaging*. 93:547–557, 2012.

5. U.S. orthopedic devices market to witness massive growth over 2017-2024. At <https://www.odtmag.com/contents/view_online-exclusives/2018-05-09/us-orthopedic-devices-market-to-witness-massive-growth-over-2017-2024/>.Accessed December 4, 2019.

6.Imaging for osteoarthritis: An overview.at <https://www.hss.edu/conditions_osteoarthritis-imaging-overview.asp>. Accessed December 4, 2019.

7. First nationwide prevalence study of hip and knee arthroplasty shows 7.2 million Americans living with implants. at <https://www.mayoclinic.org/medical-professionals/orthopedic-surgery/news/first-nationwide-prevalence-study-of-hip-and-knee-arthroplasty-shows-7-2-million-americans-living-with-implants/mac-20431170>. Accessed December 2, 2019.

8. Gazibara, T., I. Kurtagic, D. Kisic-Tepavcevic, S. Nurkovic, N. Kovacevic, T. Gazibara, and T. Pekmezovic. Falls, risk factors and fear of falling among persons older than 65 years of age. *Psychogeriatrics*. 17:215–223, 2017.

9. Complications after total knee replacement surgery.at<https://www.gponline.com/complications-total-knee-replacement-surgery/musculoskeletal-disorders/musculoskeletaldisorders/article/1209527>. Accessed December 4, 2019.

10. X-ray may be the best screening tool for diagnosing knee pain. at <https://www.health.harvard.edu/pain/x-ray-may-be-best-screening-tool-for-diagnosing-knee-pain>. Accessed December 2, 2019.

11. Hip replacement, hospital for special surgery.at <https://www.hss.edu/condition-list_hip-replacement.asp>. Accessed December 4, 2019.

12. Kataoka, M. L., M. G. Hochman, E. K. Rodriguez, P.-J. P. Lin, S. Kubo, and V. D. Raptopoulos. A Review of Factors That Affect Artifact from Metallic Hardware on Multi-Row Detector Computed Tomography. *Current Problems in Diagnostic Radiology*. 39:125–136, 2010.

13. Lee, M.-J., S. Kim, S.-A. Lee, H.-T. Song, Y.-M. Huh, D.-H. Kim, S. H. Han, and J.-S. Suh. Overcoming Artifacts from Metallic Orthopedic Implants at High-Field-Strength MR Imaging and Multi-detector CT. *RadioGraphics*. 27:791–803, 2007.

14. Leme, L. E., M. Sitta, M. Toledo., and S. da Silva Henriques. Orthopedic Surgery Among The Elderly: Clinical Characteristics. *Revista Brasileira Ortopedia*. *46*: 238–246, 2015.

15. LeVine, H. Medical Imaging. Santa Barbara: Greenwood, 2010, 95-103 pp.

16. Markatos, K. N., M. N. Sgantzos, and G. N. Tsoucalas. Hallmarks in the History of Orthopaedic Implants for Trauma and Joint Replacement. *Acta medico-historica Adriatica*. 14:161–176, 2016.

17. Mushtaq, N., K. To, C. Gooding, and W. Khan. Radiological Imaging Evaluation of the Failing Total Hip Replacement. *Frontiers in Surgery*. 6: 35, 2019.

18. Total hip replacement (THR).at <https://www.nhs.uk/conditions/hip-replacement/>. Accessed December 3, 2019.

19. Pregnancy, breastfeeding and bone health.at <https://www.bones.nih.gov/health-info/bone/bone-health/pregnancy>. Accessed December 3, 2019.

20. Potapova, I. Functional Imaging in Diagnostic of Orthopedic Implant-Associated Infections. *Diagnostics*. 3:356–371, 2013.

21. Rabin, D. N., C. Smith, R. A. Kubicka, S. Rabin, A. Ali, J. R. Charters, and H. Rabin. Problem prostheses: the radiologic evaluation of total joint replacement. *RadioGraphics*. 7:1107–1127, 1987.

22. Ribeiro, M., F. J. Monteiro, and M. P. Ferraz. Infection of orthopedic implants with emphasis on bacterial adhesion process and techniques used in studying bacterial-material interactions. *Biomatter*. 2: 176–194, 2012.

23. Ratliff, A. H. C. Ernest William Hey Groves and His Contributions to Orthopaedic Surgery. *Bristol medico- chirurgical Journal*. 98:98–103, 1983.

24. Razek, A., N. Fouda, N. Elmetwaley, and E. Elbogdady. Sonography of the knee joint. *Journal of Ultrasound*. 12:53–60, 2009.

25. Zilberman, M., and J. Elsner. Antibiotic-eluting medical devices for various applications. *Journal of Controlled Release*. 130:202–215, 2008.

ERROR ANALYSIS OF MRI DUE TO THE IMAGE RECONSTRUCTION PROCESS

Rasean Hyligar
rhylig2@uic.edu

Abstract

Magnetic Resonance Imaging (MRI) utilizes strong magnets and radio wave pulses to interact with the human body's natural magnetic properties. This allows for the better viewing of organs and tissues. While MRI is a very useful imaging tool, it is far from perfect. It has a few shortcomings that can make MRI not a valid option for some. This paper will delve into the issues that MRI has in terms of the process of reconstructing an image. As with all modern medicine and imaging practices, efficiency is key, and MRI is no exception. The problem therein is that efficiency is usually correlated with speed. While this is true, with greater speed generally comes decreased accuracy and this is one of the challenges faced by MRI machines today. With the speed that the MRI is operating at, quality loss is guaranteed to occur. This will play a detrimental role in the later steps of reconstructing the image as the initial image will have a variety of issues such as, but not limited to blurriness from movement, lower quality initial image resulting in even lower respective quality reconstruction which could lead to the diagnosis of false positives and negatives.

Keywords: *MRI, Error, Radio Waves, Relaxation, Artifacts, Imaging, Hydrogen, Protons*

1. Introduction

Before discussing the error analysis of magnetic resonance imaging (MRI), it is important to understand the physics behind MRI. In 1973, the MRI machine was first discovered by Paul Lauterbur. Lauterburg and his colleague, Peter Mansfield both received the Nobel Prize for Medicine for this invention. MRI works by taking advantage of the properties of hydrogen molecules in water, lipids and various tissues. Depending on the number of protons in a certain area will dictate the images' intensity. How the MRI uses these molecules will be discussed in the next section.

1.1 Positives of MRI Compared to Other Imaging Techniques

With the various imaging techniques available, including but not limited to, X-ray, Computed Tomography(CT), and Positron Emission Tomography (PET), MRI is the preferred option due to certain qualities it possesses. MRI does not emit ionizing radiation like an X-ray would. It uses magnets and altering of proton spins to produce an image. Secondly, images can be obtained in either a 2D or 3D plane. An example of a 2D scan of the brain can be seen in Figure 1. Imagine a breast cancer tumor. Depending on its location, a simple XY-plane search may not suffice. Depending also on the size of the slice in the x and y planes, the tumor could be completely obscured. However, doing the same scan in 3 dimensions, adding the z-component, will allow for more accurate measurement and detection**.**

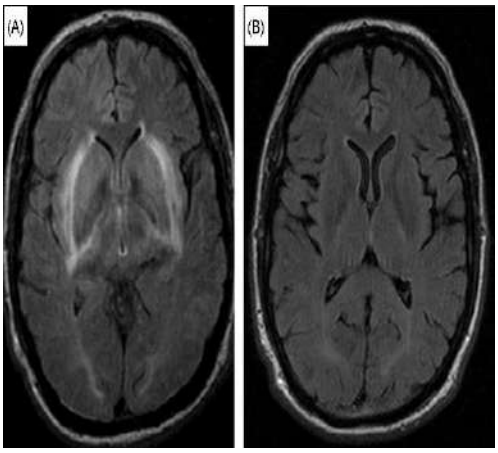

Figure 1. MRI Scan of the Brain [6]

When using MRI, the contrast between what is desired and everything else such as soft tissue, has excellent contrast. Compare this to something like X-ray, where it is much harder to distinguish between the different layers since everything is in grayscale. MRI can also be used in a multitude of parts in the human body. Ranging from neurological to musculoskeletal, because the human body contains protons everywhere, an MRI can be used in a variety of locations. There are not all the positives but merely a few to understand the power of this imaging technique.

1.2 Negatives of MRI Compared to Other Imaging Techniques

However, not every imaging technique is perfect, and MRI certainly has its downfalls. Firstly, the cost. MRI scans are significantly more expensive than CT or Ultrasound. Secondly, are the patients. By this, it means that of the patients that are admitted to having an MRI done, a large percentage of them have some sort of metallic implants. Seeing that the MRI is essentially a giant rotating magnet, one can see the dangers of someone having a metal implant and being placed into this machine. Finally, the crux of this paper, the image acquisition process. Not only is the process of obtaining the image slow, but the process of obtaining the images has differing levels of contrast between each scan taken.

Now that a brief history of MRI has been established and the pros and cons have been revealed, in the following section, we will delve deeper into the cons of the image acquisition and reconstruction process and results.

2. Image Reconstruction: A Discussion

2.1 Background of MRI and How it Works

As previously stated, here the image acquisition process will be discussed and analyzed along with the pros and cons weighed.

To begin, how is the image acquisition done on MRI machines? MRI's capitalize on the fact that humans are primarily made up of water. Water is made up of two hydrogen atoms and one oxygen atom. The hydrogens are positively charged and act like little magnets. It is also important to note that they are spinning in a seemingly random direction. This spin is calculated by using the Larmor frequency,

$$\omega = \gamma B_0 \qquad (1)$$

where γ is equal to the gyromagnetic ratio and 'B' relates to the strength of the magnetic field. When a person is exposed to an MRI machine, what happens is electricity is shot through copper coils in the machine that allow for the effect of a magnet to occur inside the machine. This causes the protons to line up via a process called relaxation. During this process, protons are knocked on their side and some even change their energy level. This is calculated by using the flip angle formula[8].

$$\alpha = \gamma B_1 \tau_{B1} \qquad (2)$$

In this formula, τ_{B_1} represents the time that the RF field pulse is turned on. The angle that they flip to determines its' energy state and if it is a T1 or T2 relaxation. A T2 relaxation is when a proton remains in a state of high energy but changes the axis on which it spins and is calculated using equation 3. A T1 relaxation is when the protons' axis is changed but unlike a T2, the level of energy reduces from high to low.

$$M_{xy} = M_0 e^{-t/T2} \qquad (3)$$

The key point of relaxation is the return of the proton from an excited state to one of equilibrium. The energy release talked about previously is what the MRI reads in order to get the image, which can then be read by a specialist.

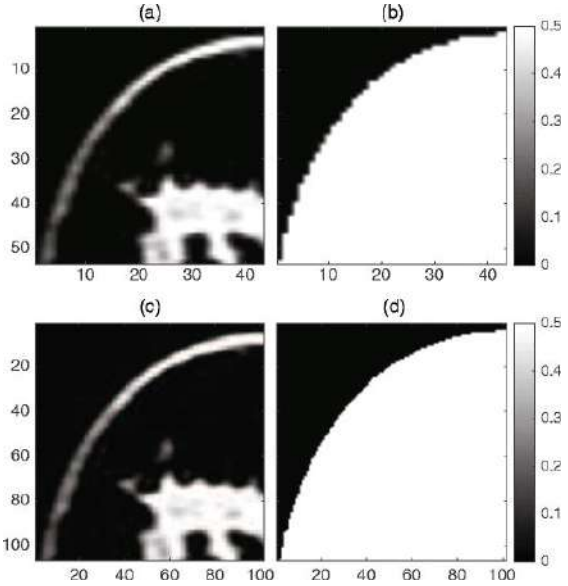

Figure 2. Oversampling effect on the intensity of voxels. (a) is a raw MRI scan and (c) is an oversampled scan of (a). The corresponding masks of (a) and (c) are (b) and (d). Masks help to identify the region accurately. The more accurate the mask, the more accurate the diagnosis. [9]

Here lies the issue with MRI. Even though this machine is accurate, there is still room for error when the machine is trying to stitch together an image. The main concern with MRI image acquisition is image artifacts. What is an artifact? An artifact is an undesired effect in an image. It is a feature in the image that is not present in the original imaged object. Some examples of artifacts in an MRI scan can be seen in Figure 3. The artifacts are labelled with arrows. The three main causes of image artifacts are patient caused, software caused, and hardware caused. Before the discussion takes place, note that the listed reasons for error in MRI image acquisition are not the only reasons.

2.2 Patient Caused Reasons

Let us begin with the patient caused reasons. One such artifact is motion artifacts. It is one of the most common artifacts and is caused by the patient moving during the scan [11]. This is usually inevitable as these scans take some time. When scanning, an MRI usually scans in segments some Δ thick, where Δ is a very small distance, usually in the micrometer area of measurement. If the scan is a relatively quicker one and depending on the scan location, this may not be the most prevalent issue. But some inevitable movements of the body such as breathing and the heart beating cannot be stopped just to take a scan and these can also cause artifacts in the form of ghosting, which a faint shadow of a previous state of a certain, in this case, organ. For example, seeing the same image of a heart where one images would appear more greyscale because that was on the intake of blood is an example [1]. One may say that a remedy can be to make the MRI stronger to make the protons stay in their flipped orientation. This is possible, but then comes the question of how strong, as placing humans into relatively powerful MRI machines yielded some harsh side effects. There are a couple main ways to remedy this. The specialist can 1) immobilize the patient before the scan takes place, or 2) set the scan to be done with a shorter phase encoding direction to reduce the amount being scanned at one time.

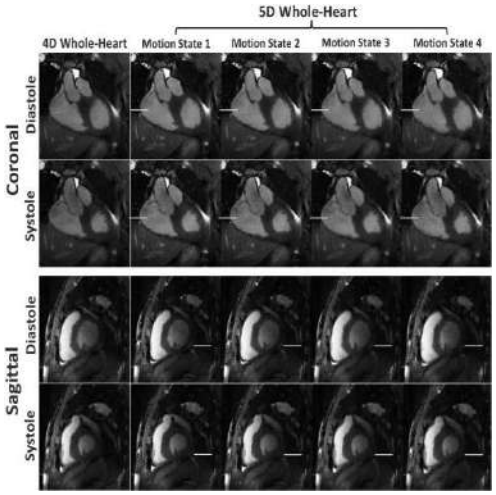

Figure 3: This is a 5D MRI of the heart. Observing the diastolic and systolic images on the top, Diastolic images have more grey color overall compared to the systole images. This is an example of involuntary movement that can be picked up by MRI that can skew the overall image [1].

The second main reason contributing to patient caused artifacts is metal [4]. What makes metal so dangerous around MRI machines is the that, as previously stated, the MRI is a giant magnet and metal is attracted to magnets. Metal can cause signal loss before or during a scan and image distortion. Assuming there are no large metal objects in

the room like chairs or cabinets that can be sucked into the MRI while it is running, since this could lead to an undesirable outcome, small implants usually can be dealt with in a variety of manners. Usually, the direction of the scan will be altered to scan along the direction that the implant is facing. This will decrease the amount of interference that the MRI will endure. Also, there is a technique known as the Metal Artifact Reduction Sequence or MARS [7]. Using MARS applies another gradient to the scan that specifically looks for metal and applies a counter frequency to that of the metal which decreases the metal interference in the scanning process.

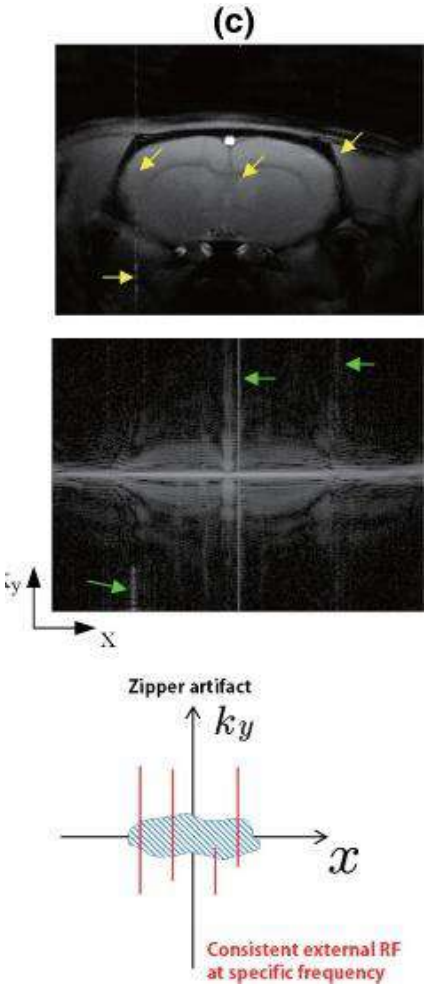

Figure 4. Examples of a motion artifact in an MRI scan. This is one of the patient caused reasons for error in the image reconstruction process. This specific one is called a zipper artifact [5]

2.3 Software Caused Reasons

There is also software caused reasons that can result in image artifacts. They are all signal processing errors. One of which can be a chemical shift [12]. Because of the differing chemical makeup and state of matter, protons in fat vibrate different to protons in water, and this can be boundary can be problematic in terms of image recreation. To remedy this, nothing can be done during the scan, however after the scan, swapping gradient filters of the scanned image and looking for a shift in the image can show whether there is an artifact or not [2]. Another software reason can be attributed to aliasing or wrap-around. This can be seen in Figure 4. The JogSSR row, row 4, has a different representation in every plane when compared to the other 3 axxed images. Usually this happens as a result of a mis-map, meaning some sort of displacement. This can usually be fixed by oversampling. An example of what oversampling looks like can be seen in Figure 2. Oversampling is taking more samples than what is needed at a higher sampling rate making it twice as fast [9].

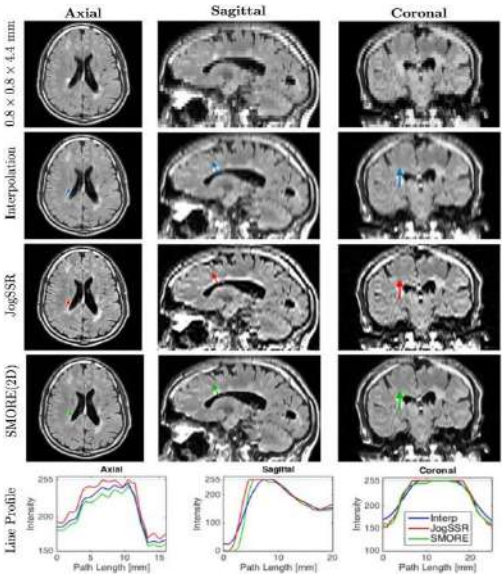

Figure 5. Example of Aliasing Effects. JogSSR has the negative effects of aliasing because it was not anti-aliased. Compare this to the results of the SMORE graph, and the effects become more clear. The line profiles are plotted based on where the corresponding color arrows are pointing on the images. [12]

2.4 Hardware Caused Reasons

Finally, some error in image acquisition is due to hardware defects and issues. One issue with hardware could be Radiofrequency (RF) quadrature. This means that when the MRI is going to be used, there is a circuit failure from incorrect operation. Usually, the only way to remedy this is to call an MRI service technician.

Another problem could be issues with the magnetic field produced. As said before, MRI use copper coils to produce the magnetic field used to interact with the human body in order to form the images. Well, this is done under some assumptions such as the magnetic field needing to be homogenous throughout. This means that the amount of Gauss or Tesla, both units used when referring to MRI or magnets, should be the same no matter where it is measured in the area of testing. If this assumption is incorrect, this results in external field inhomogeneity. This will cause a distortion in the image through spatial distortion, intensity distortion, or both. Usually, this should also require a specialist to come and assess the machine as an inhomogeneous magnetic field will never yield accurate results as a field of B_0 will never have the same amount of strength as a field with $B_0 \pm \Delta$. Finally, there are various kinds of RF noise. Every signal generates noise. Therefore, Signal-to-Noise ratio (SNR) is in existence. SNR is a ratio that is used to measure the desired signal against the noise generated. The larger the value of the SNR, the better the quality of the signal. To reduce the noise in a system, an appropriate mode of action would be to have RF shielding in place to negate the effects of wandering RF signal which would disrupt the image generation process[3,12].

3. Conclusion

To conclude, MRI machines are a fantastic feat of technological and scientific prowess. They demonstrate the power of proton manipulation via magnetization to generate images and while they are extremely powerful machines with great imaging capabilities, they are not without their caveats. We looked at how MRI images are skewed through the three main mediums of patients, hardware and software. When it came to the patient, even simple actions such as a twitch or a heartbeat can cause image acquisition discrepancies. When it came to hardware, errors in how the MRI operated in areas such as the RF coils and B_0 field were discussed, and when it came to software, changing directions of scanning or applying additional filters to compensate for undesirable effects seemed to be the most efficient route.

4. References

1. Feng, L., S. Coppo, D. Piccini, J. Yerly, R. P. Lim, P. G. Masci, M. Stuber, D. K. Sodickson, and R. Otazo. 5D whole-heart sparse MRI. *Magnetic Resonance in Medicine.* 79:826-838, 2018.

2. H. D. Park, S. P. Cho, K. J. Lee, and Y. C. Park. Minimization of gradient artefacts in cardiac-MRI-gating using adaptive interference cancellation filter with synthesized reference. *Electronics Letters*. 43:1070-1071, 2007.

3. Hansen, M. S., and P. Kellman. Image reconstruction: An overview for clinicians. *Journal of Magnetic Resonance Imaging* 41:573–585, 2014.

4. Hargreaves, B., P. Worters, K. Pauly, J. Pauly, K. Koch, and G. Gold. Metal- Induced Artifacts in MRI. AJR 197:05/05/20-547-555, May 2020.

5. Jin, K. H., J. Um, D. Lee, J. Lee, S. Park, and J. C. Ye. MRI artifact correction using sparse + low-rank decomposition of annihilating filter-based hankel matrix. *Magnetic Resonance in Medicine*. 78:327-340, 2017.

6. Kumar, G. and M. K. Goyal. Lentiform Fork sign: A unique MRI picture. Is metabolic acidosis responsible? *Clinical Neurology and Neurosurgery*. 112:805-812, 2010.

7. Kwon, Y., M. H. L. Liow, D. Dimitriou, T. Tsai, A. A. Freiberg, and H. E. Rubash. What Is the Natural History of "Asymptomatic" Pseudotumors in Metal-on-Metal Hip Arthroplasty? Minimum 4-Year Metal

Artifact Reduction Sequence Magnetic Resonance Imaging Longitudinal Study. *The Journal of Arthroplasty*. 31:121-126, 2016.

8. Nave, R. Larmor Frequency at http://hyperphysics.phy-astr.gsu.edu/hbase/Nuclear/larmor.html

9. Omer, M., and E. C. Fear. Automated 3D method for the construction of flexible and reconfigurable numerical breast models from MRI scans. *Medical & Biological Engineering & Computing* . 56:1027–1040, 2017.

10. Roberts, N. T., D. Hernando, J. H. Holmes, C. N. Wiens, and S. B. Reeder. Noise properties of proton density fat fraction estimated using chemical shift–encoded MRI. *Magnetic Resonance in Medicine*. 80:685-695, 2018.

11. Zaitsev, M., J. Maclaren, and M. Herbst. Motion artifacts in MRI: A complex problem with many partial solutions. *Journal of Magnetic Resonance Imaging.* 42:887-901, 2015.

12. Zhao, C., M. Shao, A. Carass, H. Li, B. E. Dewey, L. M. Ellingsen, J. Woo, M. A. Guttman, A. M. Blitz, M. Stone, P. A. Calabresi, H. Halperin, and J. L. Prince. Applications of a deep learning method for anti-aliasing and super-resolution in MRI. *Magnetic Resonance Imaging*. 64:132-141, 2019.

TERAHERTZ IMAGING AND ITS APPLICATIONS IN MEDICAL IMAGING

Ashwin Koppayi
alnu6@uic.edu

Abstract

Terahertz imaging is a modality of optical imaging, that uses radiation of frequency range from 100 GHz to 10THz of the electromagnetic spectrum. It is non-ionizing and non-invasive radiation that potential applications like early detection of cancer, ex-vivo spectroscopy or imaging of tissue, in-vivo examination of tissue via spectroscopy, dental care, and blood testing. The limited penetration of the THz radiation restricts the application to dermatology and dentistry. Although terahertz radiation is nonionizing, it was found to have thermal effects like effect on cell viability when the cellular temperature increased by 3^0C on the exposure of THz radiation and biological effects like effect on the stability of DNA leading to chromosomal aberrations for a range of THz radiation. Hence there is a need for a safety guideline highlighting the effects of the THz radiation and its maximum permissible exposure for each application. Lack of standardization and other limitations has led to stop the growth of this imaging modality. However, it shows a promising future in terms of diagnostic medical imaging.

Keywords: *Terahertz radiation, non-ionizing, Biological effects, Applications*

1.Introduction

Terahertz waves were formerly referred as far infra-red waves before the 1980s. They are electromagnetic waves with a frequency of 0.1 THz-10 THz (10^{12} Hz) and wavelength of 0.1mm-1mm. Demonstration of Terahertz imaging on wet leaf drying with respect to time, sparked research in Terahertz radiation for biological and medical applications.

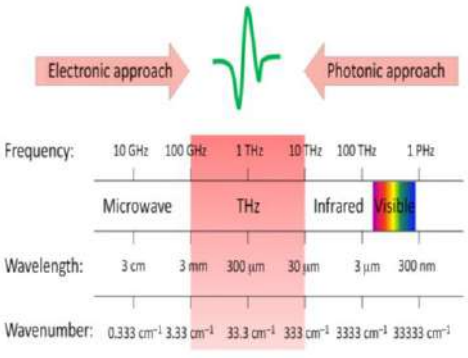

Figure 1: Terahertz range in Electromagnetic spectrum [1].

Terahertz radiation is sensitive to water content as it is strongly attenuated by water. It does not cause the ionization of biologic tissue because of its low energy millielectronvolts photons. The Terahertz radiation is sensitive to the rotational, vibrational, torsional, and conformational states. Many materials have spectral fingerprints in THz range which can used to detect these materials. These properties have led to applications of Terahertz radiation in imaging and spectroscopy [6]. Other than medical applications it is used for security screening for finding guns and explosives, atmospheric research, short range wireless communication and military applications like anti-stealth THz ultrawide radar.

2.THz Radiation System

The generation of THz radiation can be classified into two main types based on the source-electronic and photonic as shown in Figure 1. Unlike other imaging modalities like X-ray and Ultrasound, it is difficult to generate frequencies of Terahertz range by conventional electronic methods. The electronic sources are extensions of high frequency electronics and as such can only operate at the microwave end of the THz region. The upper frequency limit for electronic sources is approximately 300 GHz and they usually provide limited power at THz

frequencies. Their use is not currently widespread in medical applications. Electronic sources produce maximum frequency of 300 GHz and has low power at Terahertz frequencies which limits its application in the medical field.

By comparison, photonic sources rely on optical mixing to generate THz radiation are ubiquitous in medical applications. Narrowband continuous wave and broadband Terahertz waves can be produced by photonic sources They are used to provide both narrowband continuous wave (CW) radiation and broadband THz pulses across a wide range over a wide range of frequencies [6]. Photonic source is widely used in medical applications as it provides a wide range of bandwidth of continuous wave across a range of frequency.

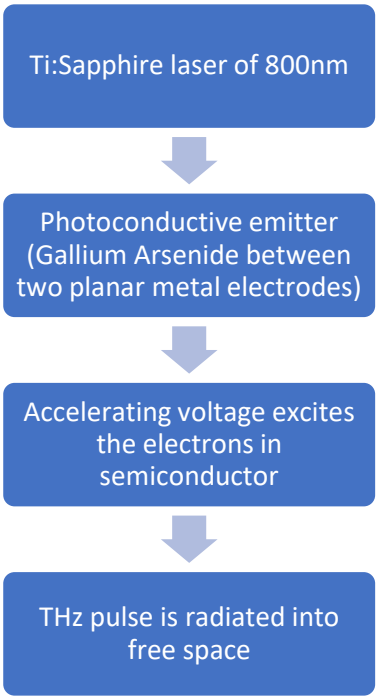

Figure 2: Block diagram of THz system for generating THz pulse.

Photoconductive emitter generates THz radiation. Emitter consists of a semiconductor crystal (Gallium Arsenide), on which two planar metal electrodes, are designed as antenna, supports a large current across the plane. Pulse of 100 femtoseconds is focused onto the gap between the electrodes. For the electrons to be excited into conduction band the energy of laser light must be above the band gap of semiconductor. Sapphire laser with a wavelength of 800nm is used to excite the electrons. Voltage is applied at one end to accelerate the excited electrons leading to rapid change in electron density. According to Hertzian dipole theory, the movement of charge causes changing dipole which produces THz pulse in the antenna that is radiated into free space [9].

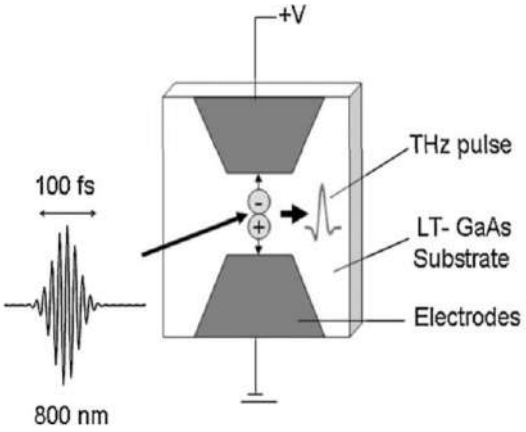

Figure 3: Generation of Terahertz Pulse radiation [7].

The Terahertz radiation is detected by photoconductive receivers. They are same as the photoconductive emitters but operates in reverse to the emitters. So, the Terahertz wave incident on the receiver accelerates the electrons and current is generated. This photocurrent is used to determine the incident Terahertz radiation [7].

3.Applications of THz Imaging

Terahertz have a wide range of application in medical imaging due to its non-ionizing and non-invasive nature. X-ray imaging fails in terms of detection of tumor without calcium deposit. THz imaging can distinguish between this kind of tumor in a nonionizing manner. Also, the energy of rotational and vibrational transitions of molecules lies in the THz region and intermolecular vibrations such as hydrogen bonds exhibit different spectral characteristics in the THz range [2]. These unique spectral features can be used to distinguish between different materials or even isomers. These unique spectral features can be used to identify materials and even isomers. This makes it suitable technique in spectroscopy for studying molecular interactions and identification of material.

3.1 Detection of Cancer

THz radiation has been applied to the imaging of

cancer tissues (The difference in the water content in a healthy tissue and malignant is used in Terahertz imaging). This difference in absorption coefficient of healthy and diseased tissue allows it to accurately differentiate boundaries between cancerous and normal tissues. It also provides invasion depth information for a cancer lesion at the initial stage. Most cancers initially start at the surface of the soft tissue. Conventional imaging modalities like Computed Tomography (CT), Magnetic Resonance (MR) is not optimal for imaging cancer on superficial tissues. Whereas Terahertz imaging provides a good contrast for detection of cancer in superficial tissues. Hence it can be used to detect cancer in early stages. THz radiation is also sensitive to the changes in hydration level and cellular structure that arise in the malignant process.

3.1.1 Brain Cancer

Brain contains high lipid content which yields a good contrast in THz imaging. Tumors contain elevated level of protein due to which absorption coefficient is high. While lipid has low absorption coefficient to THz radiation which produces a contrast in image. MR, CT and Fluoroscopy imaging is used to determine the boundary of tumor, but these techniques cannot be used while the surgery to excise tumor. Optical microscopy does not produce a proper boundary while surgery [11]. Researchers demonstrated that THz imaging can determine the boundary in animal brain tumor model as shown below.

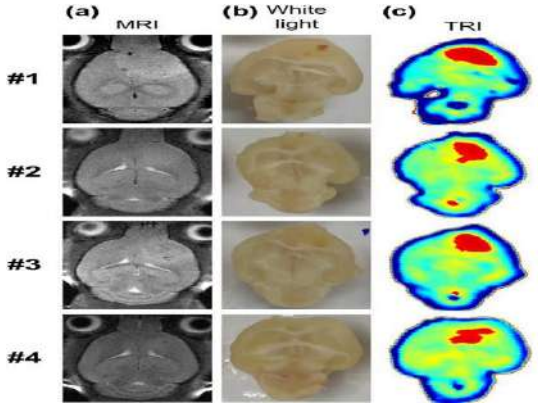

Figure 4: Image comparison of animal brain tumor model using a) MRI b) White light c) Terahertz reflection imaging [10].

Hence it has a potential to be used in clinical surgery due to accurate distinction of boundary.

3.1.2. Skin Cancer

THz imaging is useful in dermatology because of its sensitivity to water content in different skin conditions. It was previously used to study the difference between basal cell carcinoma (BCC) and normal skin in-vivo. Time domain THz pulsed imaging can also be used to find out the depth of the underlying diseased tissue. The imaging depth depends upon the wavelength of the laser used and typically ranges from 200 μm-300 μm. The lateral resolution and axial resolution of THz imaging system at 3THz is 150 μm and 20 μm which is comparable to other imaging techniques.

In-vivo studies of BCC showed good contrast when compared with the histology section of the tumor imaged. The correlation between the THz imaging and Histology section is good enough to use as a potential tool to identify the margins and depth of skin cancers [14].

3.1.3 Breast Cancer

According to American Cancer Society breast cancer is one of the most common cancer among women. It can be treated easily without chemotherapy if detected at the early stages. Currently, detection of breast cancer is either by physical examination or by Mammography. Physical examination is limited by experience of the examiner and it is used just for screening breast cancer and cannot be used to define the boundaries of the tumor [4]. Accuracy of mammography decreases with breasts size and density. Since mammography uses X-rays, it may induce malignancy.

Terahertz Imaging overcomes these limitations and is a possible means to detect breast cancer. Breast cancer detection was studied in mouse models using transmission Terahertz imaging. Cancer cells were injected in immunity compromised mice and growth of the cancer cells were observed from transmission terahertz system. The terahertz system had sensitivity to detect cancer volume of 0.05 mm^3. The color bar is defining the maximum measured T-ray absorption coefficient of cancer cells embedded in fat [3].

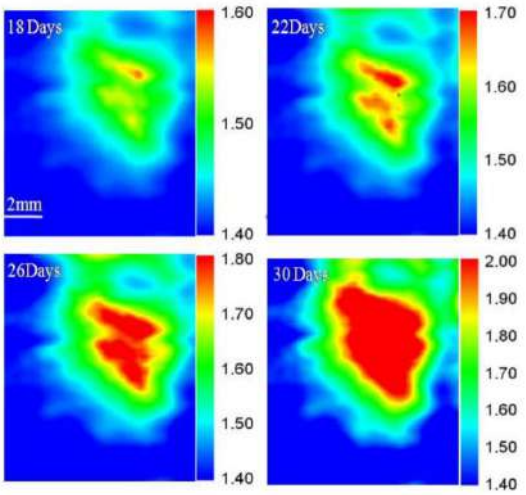

Figure 5: In vivo transmission terahertz image of mice implanted with cancer cells. Growth of cancer cells in red observed from 18-30 days [3].

In-vivo breast cancer study in humans using transmission terahertz imaging is challenging because tumors are embedded inside fibrous and fatty tissue which makes it difficult for the Terahertz waves to penetrate through it. Also, the glands present in breast have high water content which produce a similar contrast to the cancer cells [3]. These two reasons limit the use of Terahertz imaging for in vivo detection of breast cancer in humans.

3.2 In vivo spectroscopy

Terahertz imaging can be used for in vivo burn imaging. In vivo burn imaging using Terahertz imaging was studied on rats. Rat belly was imaged using THz imaging system and then it was inflicted by '+' shaped burn for 10 seconds. The burn site was reimaged every 15-30 mins till 8 hours. There is a rush of fluids in the burn site as a result of immune response which leads to edema. After 10 minutes, the region showed presence of water throughout the burned area. The unburned area reflected THz rays with same intensity as burned area. As the time passed it started to localize in the burned area and after 7 hours it could be seen that the reflectivity of the unburned area was back to normal. There is a low reflectivity area at the edges of the burned area which shows the hyperhydrated zone.

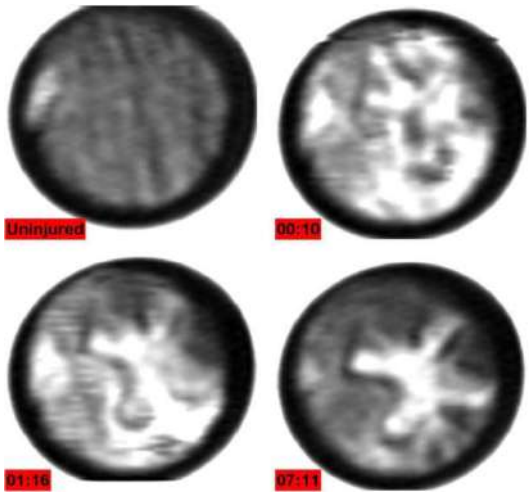

Figure 6: In vivo burn image of rat belly using reflection Terahertz imaging at different time intervals up to 8 hours [18].

Comparative study between THz and MRI for partial thickness burn showed that THz resulted in better contrast than MRI [12]. THz spectroscopy could be a powerful diagnostic tool for monitoring burn healing.

3.3. Ex vivo spectroscopy

Ex vivo spectroscopy is a potential diagnostic tool when compared with the conventional method histology. THz light can differentiate ex vivo cancerous breast tissue from a healthy tissue because of different absorption coefficient due to water content present in the tissue or cell densities. It is highly sensitive and produces a good contrast between diseased and healthy tissue. The contrast was studied by scientist who imaged dehydrated breast cancer slides using THz. The samples with carcinoma had greater reflected amplitude of THz as compared to fatty and fibrous tissue. Cell density of the samples was observed using low-power pathology photos. The carcinoma region had greater cell density which may be the reason for the contrast. They also compared the transmission mode and reflection mode of THZ imaging for characterization of breast cancer slides. It was found that transmission mode of Terahertz is less sensitive to phase change as compared to reflection which is more sensitive to phase change. This makes it difficult to accurately measure the absorption coefficient of fatty tissue. However, samples with high water content have high absorption which makes reflection mode favorable

as transmitted wave will be absorbed completely in these samples. They reported that in a transmission setup, the extraction of THz parameters is less sensitive to phase variation, so the calculation results are more robust whereas in the reflection setup, obtaining an accurate measure of absorption coefficient of fatty tissue is difficult because it is very sensitive to phase error and the flatness of the imaging window. However, reflection mode is more favorable for measuring samples with high absorption, which is true of many tissues, both excised and in vivo, due to the high-water content.

3.4 Dental Imaging

THz imaging for tooth has been investigated for more than a decade. It is a viable option for in-vivo imaging of dental carries. Carries occur due to loss of minerals from enamel and this causes a change in refractive index within the enamel. This means a small lesion which cannot be detected by eyes, can be detected. Information about the surface features using the reflection geometry THz from the outer layer of enamel can be obtained. It can be used for early detection of caries and to monitor erosion of enamel at the surface of tooth. Terahertz imaging is nonionizing and produces higher contrast unlike Xray which is ionizing and low contrast of caries. It can detect caries at early stages in the enamel layer of the teeth and monitoring of early erosion of enamel at the surface of the tooth [11]. Terahertz imaging offers a non-invasive non-ionizing alternative to x-rays and additionally provides higher contrast in clinical diagnosis.

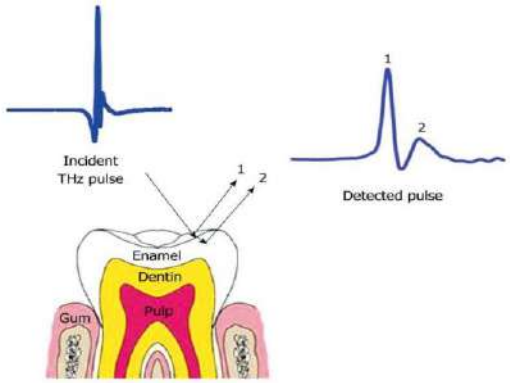

Figure 7: Detection of dental caries using Terahertz Pulse Imaging [11].

4. Limitations of THz Imaging.

The reason why THz Imaging is in infancy stage is due to low penetration depth, resolution and image acquisition. X ray and ultrasound waves have greater penetration depth as compared to Terahertz radiation. Absorption of THz radiation by water and other polar liquids limits the sensing and imaging in water rich samples and prohibits transmission mode of imaging through thick skin.

Spatial resolution of Terahertz imaging is limited by the wavelength which ranges from 1μm to 3 μm, which is not detailed enough for many medical applications. However, this can be overcome by near field imaging. In this the sample to be imaged is placed close to the aperture, a spatial resolution of a fraction of a wavelength can be achieved. The drawback of near field imaging technique is the proximity in which the sample must be placed less than 1mm for frequency of 300GHz from aperture which is not feasible for reflection mode of THz imaging.

The acquisition speed of THz image is a slow process. This is because, the image acquisition requires to move the detector in raster pattern. The image is acquired by moving the detector in a raster pattern. Alternately, array of detectors can be used but it decreases the signal to noise ratio. As an alternative to this the THz radiation can be shaped into a beam that covers the whole sample at once and an array of detector is used. However, this affects the signal to noise ratio [8].

5.Effects of THz Radiation.

THz waves can have thermal effects and non-thermal effects on biological organisms. Low energy level of THz waves overlaps of their vibration and rotational levels with biologic macromolecules demonstrate its possible application in the field of medical imaging. Like other bands of the electromagnetic spectrum, the biological effects of THz waves can be divided into thermal effects and non-thermal effects. Because of the low energy of THz waves and the overlap of their vibration and rotational levels with biological macromolecules, the nonthermal biological effects of THz radiation may demonstrate unique features and application prospects [17].

Thermal effects of THz were studied by exposing Jurkat Cell (Human T Lymphocyte) to THz waves of 2.52THz frequency continuously up to 40

minutes. Only 20% of cells survived till 40 minutes, rest of the cells underwent apoptosis. Cell viability was affected when cellular temperature was increased by 3°C and expression of heat shock proteins and DNA damage markers tend to increase when exposed to THz radiation. The levels of heat shock proteins were found to be equal in the cell exposed to THz waves for 40 mins and the cells which were exposed to high temperature. This suggests that THz radiation had thermal effect on the human cells when exposed for long time [16].

Non-thermal effects of THz waves were studied on keratinocytes and neurons. There was no change in heat shock proteins on exposing the cells to 0.14 THz wave for 80ns. Morphological changes of sensory neurons was observed in a power and wavelength dependent manner [17]. THz waves did not any effect on cell differentiation and viability of these cells.

Studies on epithelial cells, embryonic stem cells and even chromosomes had no effect on morphology, adhesion, proliferation, and differentiation on exposure to THz wave.

6. Conclusion

Terahertz imaging is a valuable technique with great potential in the medical field. It has many advantages over other imaging modalities yet due to the limitations of THz wave and lack of a proper THz system has prevented the growth of this field.

Currently, its application is limited to skin and mouth using endoscope or otoscope but, in the future, it will be used for real time imaging for determining the boundaries of tumor or cancer while surgery.

Safety concerns of using Terahertz radiation is considered the most dominant effect is thermal effect which depends on the intensity of Terahertz waves. This thermal effect is significant only if exposed for a long time and is negligible in Terahertz pulse imaging system [13].
However, the biological effects of Terahertz radiation were studied on monkey and rabbit tissues. Comprehensive study of effects on human tissue for future applications of Terahertz imaging systems is necessary.

7. References

1. Yang, X., X. Zhao, K. Yang, Y. Liu, Y. Liu, W. Fu, and Y. Luo. Biomedical Applications of Terahertz Spectroscopy and Imaging. *Trends in Biotechnology*. 34:810–824, 2016.

2. Arnone, D. D., C. M. Ciesla, A. Corchia, S. Egusa, M. Pepper, J. M. Chamberlain, C. Bezant, E. H. Linfield, R. Clothier, and N. Khammo. Applications of terahertz (THz) technology to medical imaging. *Proc. SPIE, Terahertz Spectroscopy and Applications II*. 3828, 1999.

3. Chen, H., T.-H. Chen, T.-F. Tseng, J.-T. Lu, C.-C. Kuo, S.-C. Fu, W.-J. Lee, Y.-F. Tsai, Y.-Y. Huang, E. Y. Chuang, Y.-J. Hwang, and C.-K. Sun. High-sensitivity in vivo THz transmission imaging of early human breast cancer in a subcutaneous xenograft mouse model. *Optics Express*. 19:21552, 2011.

4. Foster, R. S. Limitations of Physical Examination in the Early Diagnosis of Breast Cancer. *Surgical Oncology Clinics of North America*. 3:55–65, 1994.

5. Hintzsche, H., and H. Stopper. Effects of Terahertz Radiation on Biological Systems. *Critical Reviews in Environmental Science and Technology*. 42:2408–2434, 2012.

6. Humphreys, K., J. Loughran, M. Gradziel, W. Lanigan, T. Ward, J. Murphy, and C. Osullivan. Medical applications of terahertz imaging: a review of current technology and potential applications in biomedical engineering. *The 26th Annual International Conference of the IEEE Engineering in Medicine and Biology Society*.1302-1305 ,2004.

7. Pickwell-Macpherson, E., and V. P. Wallace. Terahertz pulsed imaging—A potential medical imaging modality? *Photodiagnosis and Photodynamic Therapy* 6:128–134, 2009.

8. Pickwell-Macpherson, E. Progress for Biomedical Terahertz Research. *The 8th International Symposium on Ultrafast*

Phenomena and Terahertz Waves, *OSA Technical Digest (online)*.2016

9. Saeedkia, D. Optoelectronic techniques for the generation and detection of terahertz waves. Handbook of Terahertz Technology for Imaging, Sensing and Communications (1rst Edition). Cambridge: Woodhead Publishing, 2013, 327 pp.

10. Son, J.-H., S. J. Oh, and H. Cheon. Potential clinical applications of terahertz radiation. *Journal of Applied Physics* .125, 2019.

11. Sun, Y. A promising diagnostic method: Terahertz pulsed imaging and spectroscopy. *World Journal of Radiology*. 3:55, 2011.

12. Taylor, Z. D., R. S. Singh, D. B. Bennett, P. Tewari, C. P. Kealey, N. Bajwa, M. O. Culjat, A. Stojadinovic, H. Lee, J.-P. Hubschman, E. R. Brown, and W. S. Grundfest. THz Medical Imaging: in vivo Hydration Sensing. *IEEE Transactions on Terahertz Science and Technology* .1:201–219, 2011.

13. Walker, G. C., E. Berry, N. N. Zinovev, A. J. Fitzgerald, R. E. Miles, J. M. Chamberlain, and M. A. Smith. An introduction to medical imaging with coherent terahertz frequency radiation. *Physics in Medicine and Biology*.47, 2002.

14. Wallace, V., A. Fitzgerald, S. Shankar, N. Flanagan, R. Pye, J. Cluff, and D. Arnone. Terahertz pulsed imaging of basal cell carcinoma ex vivo and in vivo. *British Journal of Dermatology*.151:424–432, 2004.

15. Zaytsev, K. I., K. G. Kudrin, S. A. Koroleva, I. N. Fokina, S. I. Volodarskaya, E. V. Novitskaya, A. N. Perov, V. E. Karasik, and S. O. Yurchenko. Medical diagnostics using terahertz pulsed spectroscopy. *Journal of Physics: Conference Series*. 486, 2014.

16. Zeni, O., G. P. Gallerano, A. Perrotta, M. Roman??, A. Sannino, M. Sarti, M. Darienzo, A. Doria, E. Giovenale, A. Lai, G. Messina, and M. R. Scarf,cytogenetic observations in human peripheral blood leukocytes following in vitro exposure to thz radiation: a pilot study. *Health Physics*. 92:349–357, 2007.

17. Zhao, L., Y.-H. Hao, and R.-Y. Peng. Advances in the biological effects of terahertz wave radiation. *Military Medical Research*. 1: 2014.

18. Tewari, P., C. P. Kealey, D. B. Bennett, N. Bajwa, K. S. Barnett, R. S. Singh, M. O. Culjat, A. Stojadinovic, W. S. Grundfest, and Z. D. Taylor. In vivo terahertz imaging of rat skin burns. *Journal of Biomedical Optics*. 17:040503, 2012.

POLYCYSTIC KIDNEY DISEASE (PKD): THE ROLL OF IMAGING IN DIAGNOSTIC AND CLASSIFICATION

Tarek Safieh
msafie2@uic.edu

Abstract

Polycystic kidney disease (PKD) is characterized by the formation of renal cysts in the kidneys. The two major types are autosomal dominant polycystic kidney disease (ADPKD) and autosomal recessive polycystic kidney disease (ARPKD), which play a big role in causing end-stage renal disease (ESRD) in children and adults. Certain tests detect the number and size of the cysts which can be used as one of the diagnostic tools. In this research high-resolution ultrasound, MRI, and CT scan are compared. Conventional ultrasound is currently limited by reduced diagnostic sensitivity, especially in patients younger than 30 years of age who are at high risk factor. Lately, MRI has had many impacts on trials in measuring the total kidney volume (TKV) to predict PKD progression. In comparison of MRI and CT scans for this disease, MRI is superior to CT in terms of classification and measurements because it eliminates the radiation exposure caused by CT as well as defining the cystic regions with no need of contrast agent administration. The study will show that patient with ADPKD that are evaluated by MR measures of renal and cyst volume have the most accurate and reliable measurements.

Keywords: *Polycystic kidney disease, Autosomal recessive polycystic kidney disease, High resolution Ultrasound, Total kidney volume, MRI, CT scan, Cysts*

1. Introduction

Polycystic kidney disease (PKD) is characterized by the formation of renal cysts in the kidney. Autosomal dominant polycystic kidney disease (ADPKD) is the most common inherited kidney disease and cover around 7-10% of patients on dialysis worldwide [6]. The polycystin-1 PKD1 protein is a large receptor-like protein, while polycystin-2 is a possible transient receptor vector [3]. ADPKD is the fourth cause of renal replacement therapy (RRT). The disease has been reported in the last 500 years, however, it is still untreatable and poorly understood in terms of pathogenesis approach. The rate of ADPKD vary widely between countries, rating from 4.8 in Japan to 7.9 in USA and from 3.9 to 15.3 in Europe, cases in million population per year [6]. In the past decade, the treatment and prognosis have been improved significantly in the effort of the advanced research. These cysts are noncancerous sacs containing water-like fluid that cause the kidney to enlarge and lose its function over time. Extreme cases of this disease will most likely end with an end stage renal disease (ESRD). ADPKD is still considered untreatable, proceeding persistently towards end-stage renal disease [6]. Polycystic kidney disease can also cause cysts to grow in different parts of the body like the liver and pancreas.

2. Causes and Complications

The disease is mainly caused by an abnormal gene inherited from the parents. The membrane-associated protein displays a tissue-specific pattern of expression and tends to be controlled by growth. However, in rare cases, it could be caused by a genetic mutation [2]. The two main types of polycystic kidney disease are Autosomal dominant polycystic kidney disease (ADPKD) and Autosomal recessive polycystic kidney disease (ARPKD). Many complications that are associated with PKD such as kidney failure, high blood pressure, growth of cysts in the liver, and more.

3. ADPKD Histology and Causes

ADPKD is caused by mutation in PKD1 which is responsible for 85% of cases, and PKD2 which is responsible for 15% of cases [2]. These proteins deranged activity contributes to over proliferation of tubular epithelial cells, decreased intratubular fluid secretion, and altered association between basement membrane and extracellular matrix [2].

All these modifications lead to growth of cysts. Figure 1 is a flow chart of the process of developing ADPKD from the PKD1 and PKD2.

Typical focal segmental glomerulosclerosis (FSGS) and remarkable glomerular cyst formation. Glomerular cysts produced by tubular obstruction due to misdirected filtrate distributed alongside proximal nephron tubules in patients with FSGS [5].

Glomerular cyst development may have been a characteristic of worsening FSGS. Therefore, glomerular cysts are usually seen in patients with ADPKD. The PKD researchers ' Consortium for Radiological Imaging Research (CRISP) found that the higher the total volume of the kidneys corrected for height, the quicker the predicted GFR declines [5].

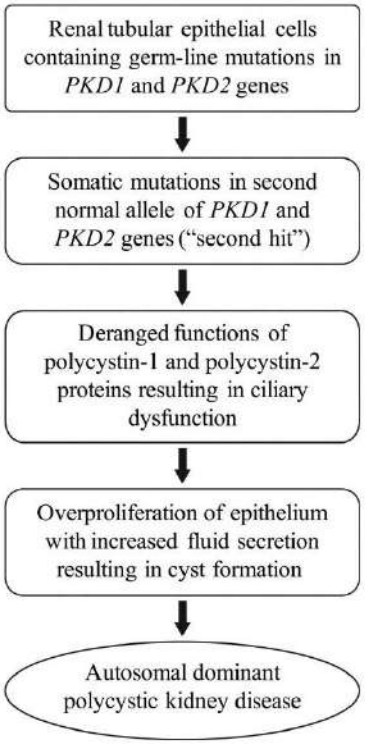

Figure 1. Flowchart illustrates the pathogenesis of the two autosomal dominant polycystic kidney disease types.

4. Ultrasound in ADPKD

Ultrasound is the initial imaging method of choice for the diagnosis of ADPKD in most patients due primarily to cost, radiation level and contrast exposure. ADPKD's disease penetration is high and ultrasound provides 99 percent sensitivity and 95 percent specificity by age 30 [1]. At ADPKD ultrasound study the kidneys appears smoothly enlarged and diffusely echogenic, this appearance is most likely caused by the many interfaces between the radially arrayed dilated ducts and the ultrasound beam [4]. Here there is a lack of corticomedular distinction, although at the periphery there may be a thin margin of hypoechoic parenchyma assumed to be compact cortex [4]. Ultrasound-based kidney volume measurements are measured using modified ellipsoid formula-based parameters.

$$\text{Kidney volume} = \text{Length} \times \text{width} \times \text{thickness} \times \pi/6 \quad (1)$$ [4].

Although ultrasonography is important for the screening and diagnosis of ADPKD, its measurement uncertainty makes it a less favored tool for tracking disease progression. Nevertheless, the retrospective evaluation of disease progression in ADPKD using ultrasound in many adults and children with ADPKD has been effective over a long period of time [1].

5. Ultrasound vs MRI Case

126 subjects ages 16-40 years born with 50% risk of ADPKD were tested [6]. The scans were performed by using L6- and C3.5 MHz or C2-5- and L4-8 MHz probes for ultrasound cyst detection. The cysts were in size between 2-3 mm in diameter and smooth back wall. In contrast, standardized respiratory-triggered, T2-weighted, axial, fat-suppressed fast-spin echo sequence without gadolinium on a 1.5 T scanner for MRI. The cysts in this method were describe sharply differentiated lesion from surrounding parenchyma with a smooth margin of at least two voxels with almost the same size that was detected by US 2.6 mm in width. Figure 3 shows a comparison between ultrasound and MRI for renal cyst around 2.5 in size [6]. Even though US is the first clinical diagnostic technique, the MRI more practical tool to rule out ADPKD. When 10 or more renal cysts are found, it is enough to diagnose with ADPKD. If five or less renal cysts are found, the subject can be considered for disease exclusion. For the HR US scanner to deliver the best results, reporting should be standardized between centers for the most accurate readings.

Figure 2. shows a small cortical renal cyst (approximately 2.5 mm) denoted by arrows in A (HR US) and B (MRI) [1].

6. CT Scan in ADPKD

At unenhanced computed tomography (CT) in ADPKD patients, the kidneys are usually flat, bloated and attenuated low, possibly representing the large volume of fluid in the dilated ducts [4]. The kidneys also show a striated pattern of contrast media excretion at excretory urography and CT when intravenous administration of contrast material is used. These striated natures of the dilated tubules reflect the deposition of contrast content [4]. In some cases, as in Budd-Chiari syndrome. a complication of liver cysts in ADPKD patient. A 59-year-old woman was diagnosed with ADPKD and hypertension at age 37 [8]. The same patient was admitted to the hospital 14 years later. Many lab work and imaging testing were done. The CT scan of the abdomen revealed multiple cysts covering almost the entire hepatic and renal parenchyma as shown in fig 4 [8]. The Doppler ultrasound showed stenosis of the inferior vena cave, with loss of the morphology of the triphasic waves in the liver superior veins. On the inferior side of the vena cava the stenosis compression was caused by the multiple cysts. That was confirmed by performing inferior vena cavography and hepatic venography by puncture of the femoral vein. From all the tests performed on the patient, the corresponding between each technique to the second is very important. That mean focusing on one single technique is not ideal and MRI, CT scan, US are all complementary to each other and can be use in such cases. CT scanning has comparable coefficients of accuracy and reliability to MRI and can be obtained much more easily than MRI. For examining complex renal cysts and nephrolithiasis, CT is also safer than ultrasound. Nevertheless, CT's drawbacks include ionizing radiation and toxicity and the use of contrast agents that are nephrotoxic [1].

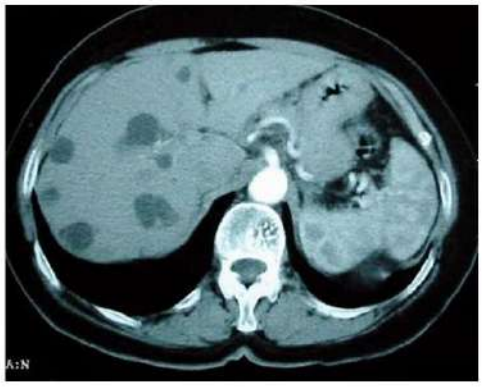

Figure 3. CT scan of the abdominal and pelvic for a patient with hepatic and kidney polycystic disease [8].

7. Conclusion

Imaging plays a major role in the treatment and control of autosomal dominant polycystic kidney disease, complication identification, and disease progression or response assessment [2]. Autosomal dominant polycystic kidney disease (ADPKD) is characterized in cross-sectional imaging by the enlargement of both kidneys by numerous cysts of varying sizes. Renal imaging is important for diagnostic and monitoring disease progression in ADPKD. Most patients with ADPKD develop renal cysts by the age of 30 years. The cysts are distributed diffusely across both kidneys, most of which have a diameter of 3 cm or more [2]. In cross-sectional imaging, cyst-associated complications such as infection, hemorrhage, and rarely cyst rupture can also be identified. In this research, MRI, CT scan, and ultrasound were compared in ADPKD diagnostic. The three imaging techniques are used to detect renal cysts; CT and MRI demonstrate better resolution and higher sensitivity for detecting renal cysts less than one centimeter in diameter. However, due primarily to cost, level of radiation and contrast exposure, ultrasound is the initial imaging modality of choice for diagnosing ADPKD in most patients [1]. In conclusion, Ultrasound currently provides the most cost-effective and reliable diagnostic approach for at risk people with ADPKD. However, in order to monitor the progression of disease over short periods of time, more accurate and reliable measures of total kidney volume such as MRI play a better roll in imaging approaches. non-cystic renal parenchyma utilizing CT could also improve the identification of ADPKD individuals at greater risk for progression to ESRD.

8. References

1. Chapman, A. B., and W. Wei. Imaging Approaches to Patients with Polycystic Kidney Disease. *Seminars in Nephrology* .31:237–244, 2011.

2. Katabathina, V. S., G. Kota, A. K. Dasyam, A. K. P. Shanbhogue, and S. R. Prasad. Adult Renal Cystic Disease: A Genetic, Biological, and Developmental Primer. *RadioGraphics*. 30:1509–1523, 2010.

3. Liebau, M. C., and A. L. Serra. Looking at the (w)hole: magnet resonance imaging in polycystic kidney disease. *Pediatric Nephrology*. 28:1771–1783, 2012.

4. Lonergan, G. J., R. R. Rice, and E. S. Suarez. Autosomal Recessive Polycystic Kidney Disease: Radiologic Pathologic Correlation. *RadioGraphics*. 20:837–855, 2000.

5. Oda, Y., N. Sawa, E. Hasegawa, H. Mizuno, M. Kawada, A. Sekine, R. Hiramatsu, M. Yamanouchi, N. Hayami, T. Suwabe, J. Hoshino, K. Takaichi, K. Kinowaki, K. Ohashi, T. Fujii, and Y. Ubara. PKD1-associated autosomal dominant polycystic kidney disease with glomerular cysts presenting with nephrotic syndrome caused by focal segmental glomerulosclerosis. *BMC Nephrology* 20: 337,2019.

6. Ong, A. C. M., O. Devuyst, B. Knebelmann, and G. Walz. Autosomal dominant polycystic kidney disease: the changing face of clinical management. *The Lancet*. 385:1993–2002, 2015.

7. Pei, Y., Y.-H. Hwang, J. Conklin, J. L. Sundsbak, C. M. Heyer, W. Chan, K. Wang, N. He, A. Rattansingh, M. Atri, P. C. Harris, and M. A. Haider. Imaging-Based Diagnosis of Autosomal Dominant Polycystic Kidney Disease. *Journal of the American Society of Nephrology*. 26:746–753, 2014.

8. Piscina, P. R. D. L., I. Duca, S. Estrada, R. Calderón, I. Ganchegui, A. Campos, K. Spicakova, L. Urtasun, M. Salvador, E. Delgado, R. Bengoa, and F. García-Campos. Combined Liver and Kidney Transplant in a Patient with Budd-Chiari Syndrome Secondary to Autosomal Dominant Polycystic Kidney Disease Associated with Polycystic Liver Disease: Report of a Case with a 9-Year Follow-Up. *Case Reports in Gastrointestinal Medicine*. 34:1–4, 2014.

9. Warner, L., M. Yin, K. J. Glaser, J. A. Woollard, C. A. Carrascal, M. J. Korsmo, J. A. Crane, R. L. Ehman, and L. O. Lerman. Noninvasive In Vivo Assessment of Renal Tissue Elasticity During Graded Renal Ischemia Using MR Elastography. *Investigative Radiology*. 46:509–514, 2011.

EVALUATING THE USE OF IMAGING TECHNIQUES IN VIRTUAL AUTOPSY FOR FORENSIC STUDIES

Sumana Mathi
mathi2@uic.edu

Abstract

Autopsy or evaluation of a body post-mortem is the most efficient way of identifying the cause of death. However, as of 2016, the rate of autopsies performed in academic hospitals in the United States hovered at around 10%. This is mainly because families refuse an autopsy for several reasons including religious or superstitious beliefs and fear of mutilation of organs of the deceased. Several methods like computed tomography and magnetic resonance imaging (CT and MRI) are being used more and more as part of scientific research in the field of forensics. Virtopsy, otherwise termed as virtual autopsy uses different imaging techniques and can provide a complete three-dimensional view of the inside and the outside of the body, along with all the required information like the depth of the wound and others that cannot be found using conventional autopsy without being destructive. Virtopsy implements modern imaging techniques into forensic sciences and aids by offering alternative methods to the existing ones. This paper aims to discuss some of the key points of virtopsy including its applications in forensics, major limitations, and future scope.

Keywords: virtopsy, virtual autopsy, magnetic resonance imaging, imaging techniques, forensics

1. Introduction

Autopsy has its origin as far back as 5000 years, in ancient Greece, Egypt and Babylon [12]. Autopsy is the conventional method that has been used to perform postmortem investigations. In deceased persons, the main objective is to analyze the cause of death, the organ affected, the depth of the wound, and manner of death along with the development of a forensic reconstruction with the findings.

Though invented several thousand years ago, the same method of autopsy is being used. A major problem to this conventional method of performing autopsies is that most families refuse an autopsy due to one of several reasons: religious and superstitious beliefs and fear of mutilation of the organs of the deceased. As of 2016, the rate of autopsies performed in academic hospitals in the United States hovered at around 10% because of the reasons stated above [13].

However, in some fields like forensic technology, there has been rapid advancement and growth in the procedures performed and technologies used. Virtopsy is one such development.

Virtopsy, or 'virtual autopsy' is extremely advantageous as it does not involve any dissection of any body cavity or of the organs of the body. Using several imaging techniques, the three-dimensional image of the body, the dimension and position of the wounds, and other vital information can be documented without the use of a scalpel unlike traditional autopsy [1].

Virtopsy was developed by Richard Dirnhofer, the former director of forensic medicine of the University of Bern, Switzerland. Thali, the forensic pathologist and project manager for Virtopsy states, "If you are doing an autopsy, you are always destroying the 3D geometry of the body. Using this cross-section imaging technique, it is possible to document the same findings in a non-invasive way" [2].

2. Autopsy vs Virtopsy

There has been a growing need for a replacement of autopsy by more efficient, non-invasive techniques. Any imaging techniques that can be used in postmortem investigative studies will, most likely, be universally accepted. Virtopsy is one huge step towards that end.

Computed tomography (CT) and magnetic resonance imaging (MRI) are used extensively in forensics to analyze the many questions that autopsy generally answers.

The "Virtopsy Project" of the Institutes of Forensic Medicine, Diagnostic Radiology, and Neurology at the University of Bern, Switzerland attempts to achieve observer-independent documentation of the body surface combined with observer-independent documentation of the interior of the body (Figure 1) [4].

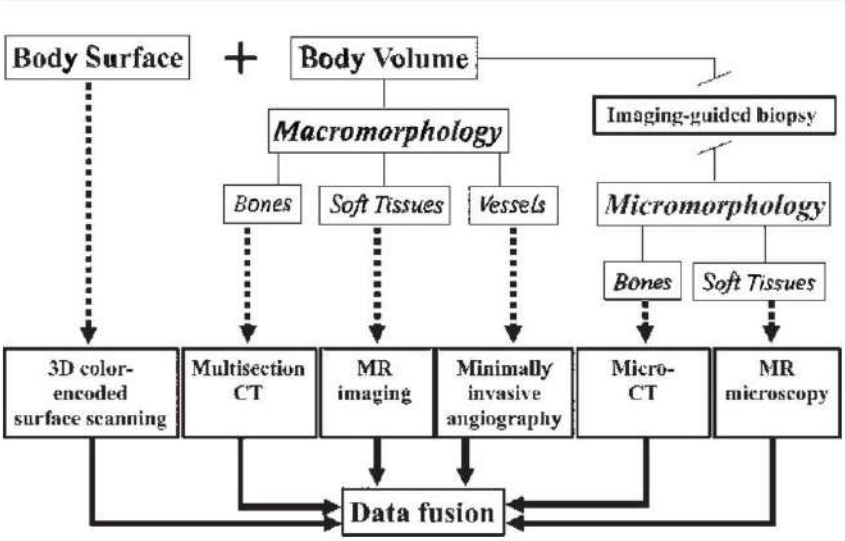

Figure 1. The Virtopsy project, in which forensic information is obtained using various radiological imaging techniques [16].

Table 1. A comparative analysis of the findings from autopsy and virtopsy through PMCT [16].

Injuries (*n*)	Autopsy		PMCT		*P*	Corrected classification
	Picked	Missed	Picked	Missed		
Scalp hematoma (18)	17	1	2	16	0.002	5.56
Skull fracture (26)	20	6	26	0	0.040	76.9
Base of skull fracture (4)	1	3	4	0	0.240	25
Facial fracture (11)	2	9	11	0	0.007	18.18
EDH (1)	0	1	1	0	0.99	0
SDH (18)	12	6	10	8	0.288	22.22
SAH (13)	13	0	2	11	0.002	15.38
Contusion (3)	2	1	2	1	0.99	33.33
Brain edema (2)	2	0	2	0	0.99	100
Cervical spine fracture (3)	0	3	3	0	0.08	0

EDH: Epidural hemorrhage, SDH: Subdural hemorrhage, SAH: Subarachnoid hemorrhage, PMCT: Postmortem computerized tomographic

The aim of the "Virtopsy project" is to validate this new method of documentation by systemically comparing the radiological and surface scanning findings with the results of conventional autopsy.

3. CT

Based on the thickness of the slice and the volume of the area to be covered, CT has been found to be extensively useful in analyzing two-dimensional and three-dimensional documentation of the following:

- Fractures
- Gross tissue injury
- Disease causing gas conditions

CT is also an excellent tool to visualize bullet tracks. Understanding the entry and exit wounds can come a long way in assisting judgements in court trials. These wounds can be determined based on the characteristic fracture pattern of the bone.

In a sample case, studied for the benefit of this paper, CT was performed on a multisection of four– or six–detector row scanners. In the study, whole-body scans were executed with a collimation of 1 or 1.25 mm. Up to 1200 axial images were obtained, with a section thickness of 1.25 mm and an increment of 0.7 mm in soft-tissue and osseous kernels. For areas of special

forensic importance, like special fracture systems, teeth, and foreign bodies, additional raw data were acquired with a collimation of 0.5 mm and 0.625-mm-thick sections were calculated. Acquisition time was approximately 10 minutes [5].

4. MRI

In a soft tissue injury, a non-traumatic pathology or a neurological and non-neurological organ trauma, MRI is the better imaging tool that can be used because it has higher sensitivity, greater specificity, and better accuracy. Currently, there has been evidence of using MRI to study child abuse victims, confirming the sensitivity of MRI for shearing injuries [14]. If these studies can be converted to a postmortem study, then there is a great scope for a non-invasive study of visceral tissue damage like cardiac or pulmonary diseases.
MRI can also be used to study the bullet tracks by determining the entry and exit wounds in not just bones, but also in soft tissues.

The following case was studied, where MR imaging of the head, thorax, and abdomen was performed on a 1.5-T system, and further areas of interest (e.g., the neck in cases of strangulation, extremities when injured) were added. Coronal, sagittal, and axial images with different contrast weighting (T1-weighted spin-echo and T2-weighted fast spin-echo sequences with and without fat saturation, turbo inversion recovery sequences and gradient-echo sequences) were acquired. Occasionally, when cardiac findings were expected or observed on axial images, short-axis, horizontal long-axis, and vertical long-axis images were acquired. Acquisition time ranged from 1.5 to 3.5 hours [6].

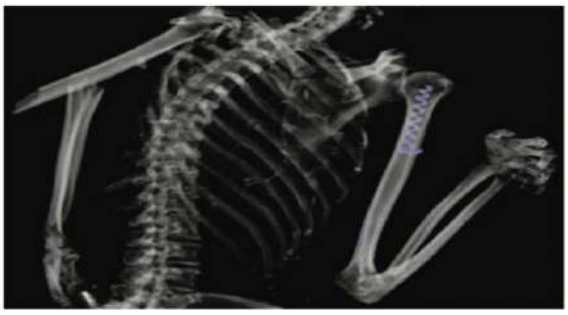

Figure 2. Corpse identification with CT- Oblique VR bone imaging obtained from a completely burnt corpse, showing a helical wire in the left humerus [15].

5. Cause and Manner of Death

a. **Brain**

Most cases of death where the brain was the fatal organ involved increased intracranial pressure. If there was a pathological finding related to an increased intracranial pressure, imaging techniques like CT or MRI can be used to analyze them and report the cause of death in forensic studies.

b. **Heart**

Putrefaction is a post-mortem alteration that can cause difficulties in conventional autopsy and virtopsy. However, it is extremely important to be able to differentiate from other kind of physiological damages to complete a forensic study. Using imaging techniques, it is possible to identify the cause of putrefaction as the formation of gases. In the heart, small gas bubbles can initially be observed via CT and these intraventricular bubbles can be seen on an MRI on low signal as well. Targeted angiography, rather than a generalized whole-body angiography, could soon become the method of choice for post-mortem analysis due to its quick imaging, affordability, and simplicity compared to the invasive autopsy techniques Figure 4.

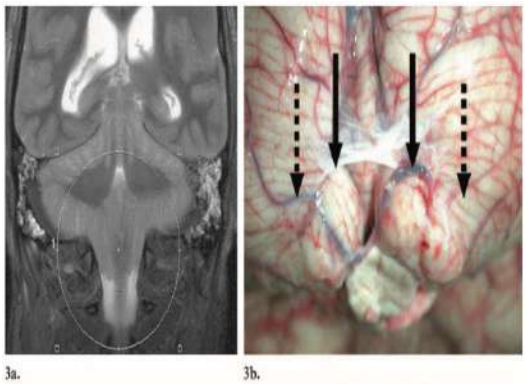

Figure 3. Comparison between virtopsy and autopsy of a image of a case where increased intracranial pressure is the cause of death. (a) MR image shows the herniation of the basilar parts of the cerebellum into the foramen magnum. (b) Autopsy shows the cerebellum with swelling of tonsils (shown by the solid arrows) and a pressure mark caused by the foramen magnum (shown by the dotted arrows) [15].

c. Lungs

To determine the cause of death, postmortem studies can access the lungs. For example, pneumothoraxes can easily be visualized using imaging techniques like CT. Pulmonary edema, which is commonly observed in several toxicological cases, can be determined using ground-glass attenuation with CT or with an increased signal attenuation in MRI as seen in Figure 5.

.

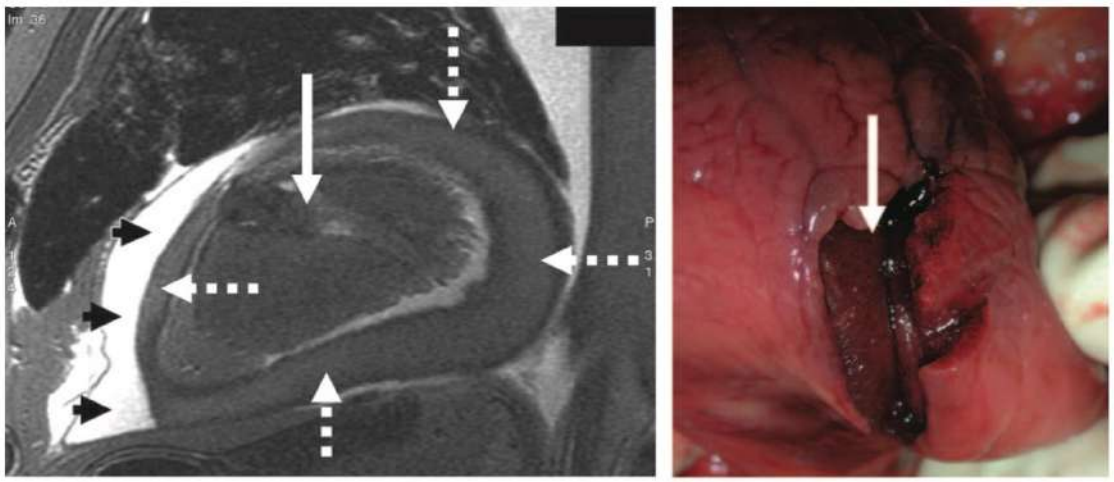

Figure 4. Cardiac trauma (stab wound to the heart). **Image on left:** MR image through the cardiac apex shows a myocardial injury (solid white arrow). Subsequent pericardial tamponade manifests as sedimented cellular components (dashed white arrows) with medium signal intensity and an upper layer of serum (black arrows) with increased signal intensity. **Image on right:** Photograph of the corresponding autopsy specimen demonstrates transmural laceration of the left ventricle in the apical region (arrow) [15].

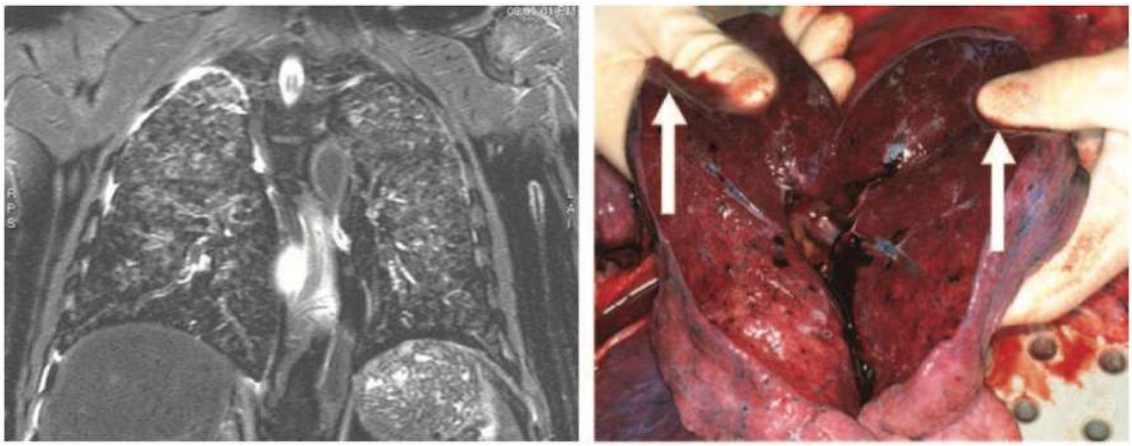

Figure 5: Pulmonary edema. **Image on left:** MR image of the thorax shows a global increase in signal intensity throughout the lungs caused by an increased fraction of intrapulmonary water. **Image on right:** Photograph of the corresponding autopsy specimen shows the loss of tissue water after sectioning. Note the accumulation of the drained edema (arrows) surrounding the thumbs of the forensic pathologist [15].

5. Vitality of Sustained Injuries

Vital studies help elucidate the sequence of injuries and death for forensic investigations. The question of if the victim was alive or dead during a incident can hold crucial information with regards to the forensic investigative studies.

a. **Trauma**

Ongoing ventilation after trauma is revealed by aspirated material – blood or gastric content. Similarly, soft tissue emphysema reveals blunt trauma. Soft tissue emphysema, after palpation, cannot be observed in an autopsy because, once the overlying skin is incised, the air will disappear. Active swallowing of foreign particles can help in demonstrating if the victim was alive during the time of the incident.

b. **Hanging**

There are several possibilities where a suicide is simulated to cover up a homicide. So forensic scientists' study vital reactions to exclude this. Bleeding into the insertions of the sternocleidomastoid muscle or soft-tissue structures of the neck prove that circulation was ongoing at the onset of strangulation, and strong breathing attempts against the occluded airways cause alveolar ruptures with subsequent pneumomediastinum and soft-tissue emphysema ascending into the neck [7].

6. Advantages

- Virtopsy is effective in studying wounds and the wounds can be matched with the probable weapon used in the murder.
- Virtopsy is a non-invasive, that is, no scalpel is used in the postmortem study and so there is no tissue damage of the body of the deceased.
- There is no mutilation of any organ of the body, unlike autopsy. So, even after virtopsy, a conventional autopsy can be performed on the body.
- Virtopsy is less time consuming as the body can be released immediately after scanning.
- Relatives of the deceased prefer virtopsy as no religious or superstitious beliefs are disturbed.

7. Disadvantages

- There is not enough database to compare autopsy and virtopsy.
- There are some pathological conditions that can be identified only with autopsy as there has not been enough advancements in imaging for some conditions yet.
- Infection status cannot be given.
- It can be difficult to distinguish between the antemortem and postmortem wounds.
- Small tissue injuries can be missed.

8. Real Data Based Forensic Reconstruction of Images

With CT data, it is possible to reconstruct images to understand the exact scenario during the incidence of the injury in the body. This enables easier investigation as the real image can be compared with reconstructed animation from the CT developed reconstruction images. The possession of such data fusion helps in answering several questions with regard to dynamic development of patterned injuries and to evaluate their match ability and link ability to the suspected instrument that caused the injury, even several years after the injury.

Figure 6 shows real data-based reconstruction of a case where a pedestrian was hit by a car. This data combined with data at hand helped in deducing that the pedestrian was on his knee when the incident happened.

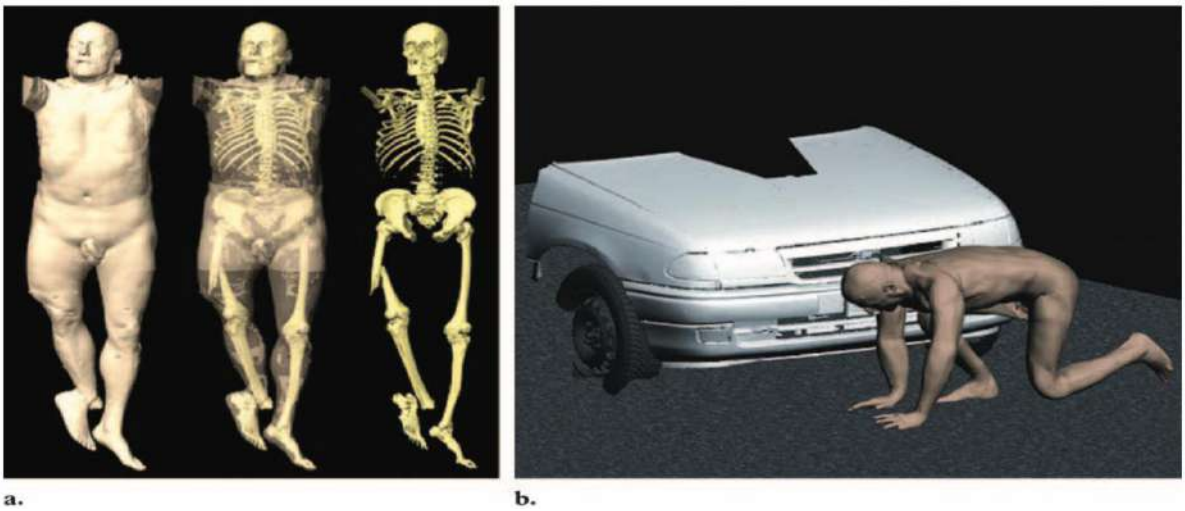

Figure 6: (a) Three-dimensional CT images show how information about joints can be used to define movable extremity models with surface details. (b) Image illustrates how correlation of the 3D surface image of the car (including the damage to the car) with the injuries of the victim allows forensic reconstruction of the accident [17].

9. Conclusions

From the review, it can be stated that imaging techniques are extremely beneficial tools in forensic science. Their main advantage being that they can freeze any data from the time of the incident without causing any kind of damage to the body of the deceased. Non-destructive techniques are extremely important for the following two reasons:

- First, they bring information without precluding any other conservative or destructive forensic investigation.
- Second, they can be used in cultures and situations where autopsy is not tolerated by religion or rejected by family members.

Virtopsy or 'virtual autopsy' is an excellent technique that can remove several existing issues with current methods, but it still has a long way to go before it can entirely replace the autopsy.

Hopefully, soon, non-invasive imaging techniques will be used by forensic surgeons to investigate and present cases in courts of justice.

10. References

1. 'Virtual autopsies may cut scalpel role at <cnn.com>. Accessed November 20, 2019.

2. The future is Virtopsy: Sequence format (Neue Zuricher Zeitung). <www.Virtopsy.com>. Accessed Dec 1, 2019.

3. Wullenweber R, Schneider V, Grumme T. A computer-tomographical examination of cranial bullet wounds [in German]. *Rechtsmed* 1977; 80: 227– 246, 1977.

4. Brueschweiler W, Braun M, Fuchser HJ, Dirn- hofer R. Photogrammetrische Auswer- tung von Haut- und Weichteilwunden sowie Knochenver - letzungen zur Bestimmung des Tatwerkzeuges , grundlegende Aspekte. *'Post-mortem computed tomography of stillborns with bone pathology*. *Rechtsmedizin*. 7: 1976 –1983, 1997.

5. Sidler M, Jackowski C, Dirnhofer R, Vock P, Thali M. Use of multislice computed tomography in disaster victim identification: advantages and limitations. *Forensic Science International*. 169: 118-128, 2007.

6. Aghayev E, Yen K, Sonnenschein M, et al. Virtopsy post-mortem multi-slice computed tomography (MSCT) and magnetic resonance imaging (MRI) demonstrating descending tonsillar herniation: comparison to clinical studies. *Neuroradiology*. 46:559 – 564, 2004.

7. LundbergGD. Low-tech autopsies in the era of high-tech medicine: continued value for quality assurance and patient safety. *Journal of the American Medical Association*. 280:1273-1274, 1998.

8. Bolliger SA, Thali MJ, Ross S, Buck U, Naether S, Vock P. Virtual autopsy using imaging: bridging radiologic and forensic sciences. A review of the Virtopsy and similar projects. *European Radiology*. 18: 273-282, 2008.

9. Ruder TD, Thali MJ, Hatch GM. Essentials of forensic post-mortem MR imaging in adults. *The British Journal of Radiology*. 87, 2014.

10. Bisset, R & Thomas, Nigel & Turnbull, I & Lee, S. Postmortem examinations using magnetic resonance imaging: Four-year review of a working service. *BMJ (Clinical research ed.)*. 324. 1423-4 , 2002.

11. Patowary, A.J. Virtopsy: One step forward in the field of forensic medicine–A review. *Journal of Indian Academy of Forensic Medicine*. 30, 2008.

12. Walker HK. The Origins of the History and Physical Examination. In: Walker HK, Hall WD, Hurst JW, editors. Clinical Methods: The History, Physical, and Laboratory Examinations. 3rd edition. Boston: Butterworths; 1990. Chapter 1.

13. Blokker BM, Weustink AC, Hunink MG, Oosterhuis JW. Autopsy of Adult Patients Deceased in an Academic Hospital: Considerations of Doctors and Next-of-Kin in the Consent Process. *PLoS One*. 11(10), 2016.

14. Mutch CA, Talbott JF, Gean A. Imaging Evaluation of Acute Traumatic Brain Injury. *Neurosurg Clinics of North America*. 27: 409–439, 2016.

DIAGNOSTIC VALUE OF WHOLE-BODY DIFFUSION-WEIGHTED IMAGING IN BREAST CANCER

Peiyao Li
pli38@uic.edu

Abstract

In recent years, due to the development of science and technology and the gradual improvement of medical level, MRI whole-body diffusion imaging equipment and related technologies in clinical medicine have achieved rapid development and progress. The images provided by diffusion weighted MRI have different tissue contrast conventional MRI and can promote patients to complete the scanning of various parts of the body, including pelvis, abdomen, chest, etc. under the condition of free breathing, and can obtain high-resolution, high signal-to-noise ratio images, and can be used for the location, scope, size, shape, etc. of lesions. DWI assesses the micro-movement of tissue water molecules, which is thought to reflect the lesion's cellular structure and membrane integrity. The DWI of malignant breast lesions is characterized by high fiber density and limited diffusion of water molecules, which helps to distinguish it from benign breast lesions. Advances in DWI acquisition and modeling methods have helped improve image quality and extract additional biological information from breast DWI scans, which may extend diagnostic and prognostic value. Therefore, the purpose of this study was to assess the diagnostic value of DWI in breast cancer. This review article provides insights in to the evolution of DWI as a new imaging paradigm and provides a summary of current role of DWI in various disease processes.

Keywords: *Diffusion weighted imaging, Breast cancer, Diagnosis, Breast lesions*

1. Introduction

About 60 - 70% of the human body is composed of water. Diffusion is a random Brownian motion driven by heat energy. In a complex human environment, water is divided between cells and extracellular compartments. Different tissues of the human body have unique cell structure and the proportion of inner and outer cells [1]. Therefore, it has special diffusion characteristics. The relative distribution of water between these chambers is affected by the pathological process. For example, in high-grade malignant tumors and acute infarction tissues, the proportion of cells increases, so the diffusion is relatively limited. Diffusion weighted imaging provides qualitative and quantitative information about diffusion characteristics. Diffusion weighted imaging (DWI) has been at the forefront of cancer imaging since the beginning of 2000 [2]. A large number of DWI studies show that the diffusion characteristics of breast malignant lesions have changed compared with normal fibrous glands. Moreover, DWI is a short scan available on most commercial MR scanners that does not require any exogenous contrast and can be easily added to clinical breast MRI protocols. Complementary information about the microenvironment and the relative ease of implementation make DWI an interesting imaging tool to improve the diagnosis and understand the characteristics of breast cancer.

2. Breast DWI Basics

DWI is used to detect diffusion characteristics in MR image acquisition using motion sensitive gradients. The strength of the resulting diffusion weighted MRI signal is directly proportional to the water mobility, which is usually described by a single exponential equation:

$$S_D=S_0e^{-b\cdot ADC} \quad (1)$$

where S_D is the signal intensity with diffusion weighting, S0 is the signal intensity without diffusion weighting, b is the b-value determined by the strength and timing of the applied diffusion gradients (s/mm^2), and ADC is the apparent diffusion coefficient [3], which describes the rate of diffusion (mm^2/s).

Due to the hindered restricted diffusion and proliferation of cells, breast cancer usually shows DWI high signal, ADC is lower than normal breast parenchyma (Fig. 1).

It is very important for doctors to accurately estimate the extent of tumor cell involvement and lymph node metastasis in the process of choosing the appropriate breast cancer operation plan. It is reported that the survival time and recurrence rate of tumor metastasis and other prognosis related indexes of patients with positive margin of focus are much worse than those of patients with a negative margin. While breast lesions tend to be most visible on the diffusion-weighted images, such images have confounding T2-shine effects and therefore most clinical applications rely on quantitative ADC measures for lesion characterization.

3. Clinical Applications

DWI is widely used in breast imaging as an auxiliary diagnostic tool of DCE-MRI to distinguish benign and malignant lesions. DWI provides a painless, convenient and effective examination method, which reveals the internal changes of the tumor at the molecular level, obviously earlier than the morphological changes. In the early stage of chemotherapy, some tumor cells are induced to necrosis, the cell membrane, and its relatively normal biological environment is restored, the ability of water diffusion inside and outside the cells is significantly enhanced compared with before, and then the ADC value is increased. However, the common indicators for daily measurement of therapeutic effects, such as tumor volume or shape, can only be displayed after the necrotic substance is absorbed and removed for a long time. Some researchers confirmed through animal experiments that DWI can monitor the early changes of breast cancer after treatment, and it is hopeful to become a new evaluation technology instead of the measurement of tumor size [reference]. Many previous studies have shown breast malignancies have significantly lower ADC values than benign lesions. Pickles [5] et al. studied 10 patients with breast cancer undergoing neoadjuvant chemotherapy before and after treatment. The ADC values before and after treatment were (1.00 ± 0.00) × 10^{-3} mm^2/s, the average value after one cycle of chemotherapy

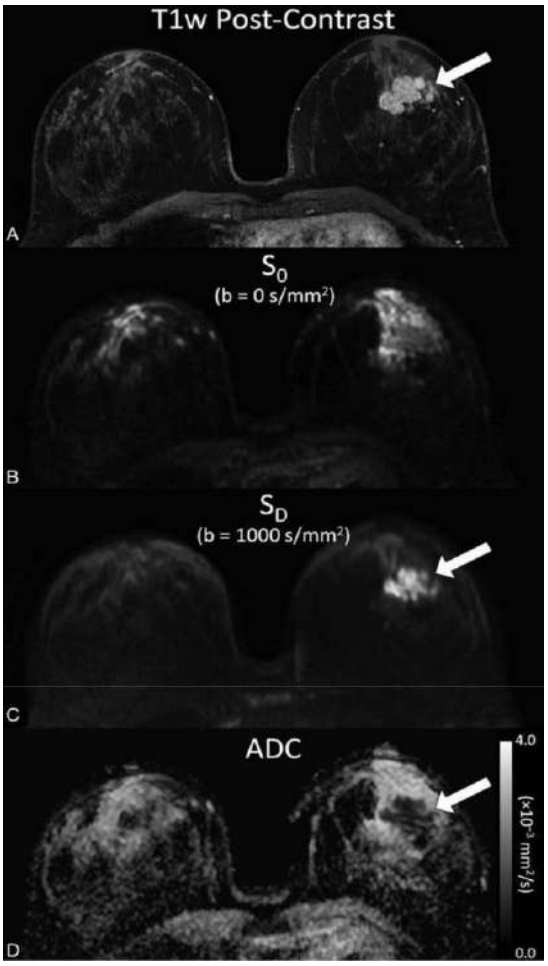

Figure 1. Example breast DWI images obtained in a 37-year-old woman with invasive breast cancer. Shown are corresponding images from (A) post-contrast T1-weighted image, (B) DWI S_0 with b = 0 s/mm^2, (C) DWI SD with b = 1000 s/mm^2, (D) apparent diffusion coefficient (ADC) map. Invasive carcinoma (arrow) exhibits reduced difusivity on DWI, appearing hyperintense on the S_D image and hypointense on the ADC map. [4]
=

was (1.14 ± 0.09) × 10 $^{-3}$ mm^2/s and rose to (1.27 ± 0.17) × 10^{-3} mm^2/s after two cycles of chemotherapy. Some studies have shown that the ADC value after treatment is higher than that before treatment after DWI examination for tumor patients with neoadjuvant chemotherapy. However, there is no significant change in the ADC value before and after treatment for some pathological types of tumors that are not sensitive to chemotherapy, and the decrease of ADC value cannot be excluded. The above conclusion can be explained by cell death and cell density of drug-sensitive tumors due to the action of drugs which give the water molecules more space to

while the tumor of drug-resistant or ineffective treatment not only does not shrink but also increases the cell density, to reduce the ADC value. Theimann RJ [6] et al. found an obvious change 4 days after the start of chemotherapy, and the most significant change occurred at 11 days.

At present, DWI has been used to study the ADC value of brain cancer, nasopharyngeal carcinoma NPC) [7] and Hepatocellular carcinoma (HCC) [8] in different periods after radiotherapy, but there are few reports on the evaluation of ADC value of breast cancer in different periods by DWI. This is related to the fact that most breast cancer patients go to breast surgery for surgical treatment, and the tumor has disappeared after preventive radiotherapy. But DWI still has an important application value for breast cancer patients who are unwilling to accept surgery, lose the opportunity of surgery or release after surgery. According to the principle of DWI imaging and the basis of pathophysiology, whether the ADC value of breast cancer lesions changes earlier than the change of its morphological volume, and whether ADC value measurement can be used as a means to judge the efficacy of breast cancer radiotherapy will have great scientific research value and development potential. At the same time, DWI may play a unique role in the evaluation and prediction of adverse reactions caused by radiotherapy because of the morphological changes of normal tissues and focus tissues, such as fibrosis and edema.

4. Evaluations and Analysis

Although more and more imaging centers include DWI in clinical breast MR examination, there are still many technical factors and analysis related to image acquisition that are considered as successful implementation. Image quality can vary greatly, so it is necessary to optimize the breast DWI acquisition protocol to reduce artifacts and achieve sufficient signal-to-noise ratio (SNR). The spatial resolution of DWI is poor, and the quality of anatomical images is far inferior to that of the enhanced scan. Only by combining enhanced images can lesions be accurately located and ADC values of lesion tissues be measured. Therefore, it cannot be applied to the diagnosis of breast diseases alone at present. In MRI diffusion imaging, ADC value error is inevitable, such as interference caused by gland hyperplasia, and overlap of ADC values measured by different pathological types, poor spatial resolution of DWI images, a magnetic sensitive artifact caused by blood perfusion, etc. Data analysis methods including post-processing, ADC calculation, and region of interest (ROI) can also directly affect ADC measurement. Image registration can be used to correct patient's motion and sensitive and eddy current related EPI distortion before ADC calculation. In the calculation of ADC, an appropriate noise threshold should be used to reduce the false value of fat tissue signal when it is suppressed [9]. According to ROI selection methods (Fig. 2), ADC measurement values of lesions were significantly different, ranging from small area sampling to the whole tumor three-dimensional ROI method [10,11].

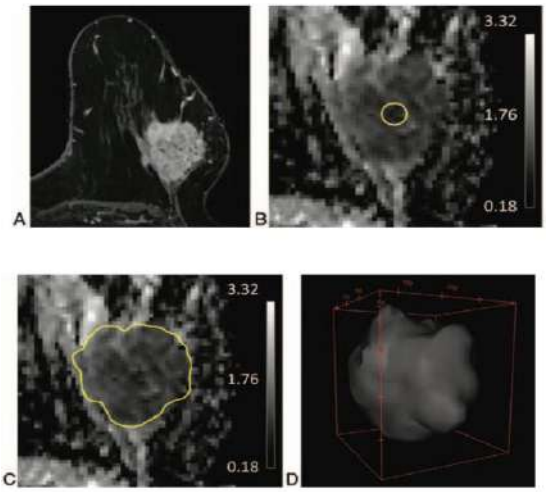

Figure 2. Illustration of varying tumor ADC measurement approaches. Shown are (A) reference T1-weighted postcontrast slice, (B) small minimum ADC subregion ROI, mean ADC = 0.65×10^{-3} mm^2/s, (C) single slice 2D whole tumor ROI, mean ADC = 0.88×10^{-3} mm^2/s, (D) 3D whole tumor ROI, mean ADC = 1.01×10^{-3} mm^2/s. As shown, choice of ROI technique can substantially affect lesion ADC measures [6].

The differences of ADC are most significant in large, heterogeneous, and non-mass lesion [9]. Some studies have reported that placing a smaller ROI in the low – intensity ADC area can reflect the worst pathology in in heterogeneous lesions, thus providing better differential performance [10, 11]. However, the whole tumor measurement may have better reproducibility. Semi-automated ROI of improving the efficiency, accuracy, and reproducibility of breast lesion ADC measure [12].

5. Advanced DWI Modeling

Although the simple single-compartment mono-exponential decay model to estimate ADC is by far the most common quantitative approach utilized in clinical DWI application, more complicated modeling techniques are under study to extract more biological information from breast DWI scans [13]. One of the methods is intravoxel incoherent motion (IVIM) modeling, which fits the DWI signal to a multi-compartment bi-exponential and surrounding substance. [14]. IVIM allows measurement of tissue

parameters, including perfusion volume fraction (f_p), tissue diffusion coefficient (D_t) in the parenchyma, and pseudo diffusion coefficient (D_p or D^*) in the microvascular system. Applied to breast cancer, D_t is considered a marker of tumor cellularity, f_p of blood volume, and D_p of blood velocity and vessel architecture (Fig. 3)
[15]. The preliminary studies of IVIM have shown that the increase of f_p levels in invasive breast cancers [16] may reflect angiogenesis related to more aggressive disease and therefore may provide additional diagnostic and prognostic value [17].

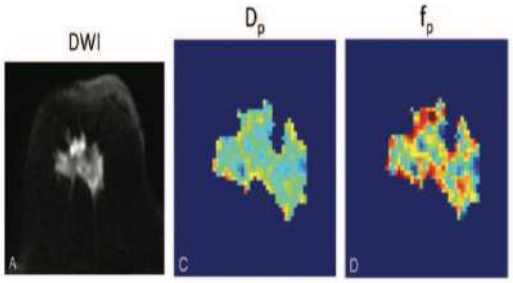

Figure 3. DWI with intravoxel incoherent (IVIM) biexponential modeling of an invasive ductalcar cinomaina 62-year-old woman. Distinct physiological information is obtained by separating the IVIM components. Shown are the (A) DWI (b = 800 s/mm^2) image and maps of the (B) tissue diffusion coefficient (D_t), (C) micro-vasculature pseudodifusion coefficient (D_p), and (D) perfusion fraction (f_p) [19].

Diffusion tensor imaging (DTI), another advanced technique, is widely used in the field of neuroimaging, which is also being investigated for application in breast imaging. DTI characterizes both the rate (diffusivity) and directionality (anisotropy) of water diffusion and it is hypothesized it may provide further study of gland tissue (ducts, lobules) and micro-architecture. The measurement of DTI anisotropy in breast lesions is usually lower than that in normal parenchyma, which is considered to reflect the loss of gland tissue in the lesions (Fig. 4), which is thought to reflect the loss of glandular tissue in the lesions, and some studies have also reported lower anisotropy values in benign versus malignant lesions [18].

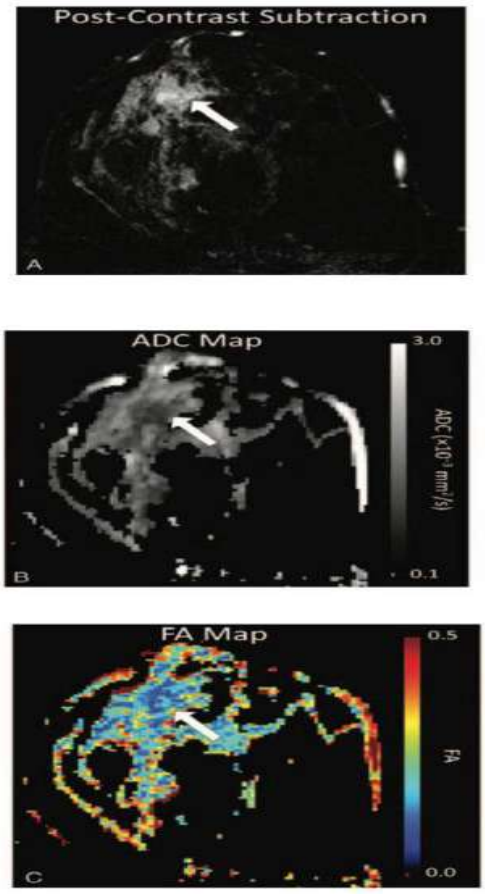

Figure 4. Example of DTI in a 34-year-old woman with invasive ductal carcinoma. Shown are (A) postcontrast T1-weighted subtraction image, (B) ADC map, and (C) fractional anisotropy (FA) map. The enhancing tumor (arrow) exhibits restricted diffusion with reduced ADC (ADC = 0.94 × 10^{-3} mm^2/s) and anisotropy (FA = 0.12) versus nearby normal parenchyma, suggesting increased cell density and loss of structured organization [19].

6. Conclusion

As more physicians realize the potential value of DWI in the diagnosis and treatment of breast cancer, and this auxiliary MRI technology will be included in the breast MRI program. DWI has a special appeal because of its short acquisition time, wide availability on most commercial MR scanners, and no need to inject exogenous contrast agents. However, there is no uniform standard for the two most important parameters b-value and ADC of DWI. The discussion of b-value optimization and the determination of ADC threshold for the differentiation of breast lesions with different properties have been a hot topic for scholars all over the world.

DWI is the product of the rapid development of molecular imaging technology. Researchers believe that DWI is still not reaching its full potential and one day it may be able to solve the most complex puzzles in breast cancer detection.

7. References

1. Baliyan V., Das J.C., Sharma R., Gupta K.A. Diffusion weighted imaging: Technique and Applications. *World Journal of Radiology*. 8: 789-798, 2016.

2. White N., McDonald C., Farid N., et al. Diffusion-weighted imaging in cancer. Physical foundations and applications of Restriction Spectrum Imaging: *Cancer Research.* 74: 4638-4652, 2014.

3. Le Bihan D., Breton E., Lallemand D., al. MR imaging of intravoxel incoherent motions: application to diffusion and perfusion in neurologic disorders. *Radiology*. 161: 401-407, 1986.

4. Partridge S.C., McDonald E.S. Diffusion weighted magnetic resonance imaging of the breast: protocol optimization, interpretation, and clinical applications. *Magnetic Resonance Imaging Clinics of North America*. 21: 601-624, 2013.

5. Pickles M., Gibbs P., et al. Diffusion changes precede size reduction in neoadjuvant treatmerit of breast cancer [J]. *Magnetic Resonance Imaging*. 24: 843-847, 2006.

6. Theilmnn R.J., Borders R., et al. Changes in water molilty measured by diffusion MRI predict response of metastatic breast cancer to chemotherapy[J]. *Neoplasia*. 6: 821-837, 2004.

7. Wang C., Liu L., Lai S., Danke S., et al. value of diffusion-weighted magnetic resonance imaging for local and skull base recurrence of nasopharyngeal carcinoma after radiotherapy. *Medicine*. 29: e11929, 2018.

8. Gluskin S.J., Chegai F., Monti S., Squillaci E. and Mannelli L. Hepatocelluar Carcinoma and Diffusion-Weighted MRI: Detection and Evaluation of Treatment Response. *Journal of Cancer*. 7: 1565-1570, 2016.

9. Partridge S.C., Nissan N., Rahbar H., et al. Diffusion-weighted breast MRI: clinical applications and emerging techniques. *Journal of Magnetic Resonance Imaging*. 45: 337-355, 2017.

10. Le Bihan D, Breton E, Lallemand D, et al. separation of diffusion and perfusion in intravoxel incoherent motion MR imaging. *Radiology*. 168: 497-505, 1988.

11. Bokacheva L., Kaplan J.B., Giri D.D., et al. Intravoxel incoherent motion diffusion-weighted MRI at 3.0T differentiates malignant breast lesions from benign lesions and breast parenchyma. *Journal of Magnetic Resonance Imaging*. 40: 813-823, 2014.

12. Rahbar H., Kurland B.F., Olson M.L., et al. Diffusion-weighted breast magnetic resonance imaging: a semiautomated voxel selection technique improves interreader reproducibility of apparent diffusion coefficient measurements. Journal of Computer Assisted Tomography. 40: 428-435, 2016.

13. Arponen O., Sudah M., Masarwah A., et al. Diffusion-weighted imaging in 3.0 Tesla breast MRI: diagnostic performance and tumor characterization using small subregions vs. whole tumor regions of interest. *PLoS One*. 10: e0138702, 2015.

14. Ahlawat S., Khandheria P., Del Grande F., et al. Interobserver variability of selective region-of-interest measurement protocols for quantitateve diffusion weighted imaging in soft tissue masses: comparison with whole tumor volume measurements. *Journal of Magnetic Resonance Imaging*. 43: 446-454, 2016.

15. Bickel H., Pinker K., Polanec S., et al. Diffusion-weighted imaging of breast lesions: Region-of-interest placement and different ADC parameters influence apparent diffusion coefficient values. *European Radiology*. 27:1883-1892, 2017.

16. Iima M., Yano K., Kataoka M., et al. Quantitative non-Gaussian diffusion and intravoxel incoherent motion magnetic resonance imaging: differentiation of malignant and benign breast lesions. *Investigative Radiology*. 50: 205-211, 2015.

17. Liu C., Liang C., Liu Z., et al. Intravoxel incoherent motion (IVIM) in evaluation of breast lesions: comparison with conventional DWI. *European Journal of Radiology*. 82:782-789, 2013.

18. Tsougos I., Svolos P., Kousi E., et al. The contribution of diffusion tensor imaging and magnetic resonance spectroscopy for the differentiation of breast lesions at 3T. *Acta Radiologica*. 55:14-23, 2014.

19. Partridge S., Amornsiripanitch N. DWI in the assessment of breast lesions. *Topics in Magnetic Resonance Imaging*. 26: 201-209, 2017.

Mission Statement and Bylaws - Spring 2016

Mission

The mission of the journal is to develop the art of scientific writing among bioengineering students. Students may submit articles that describe original research or that review existing research (with proper credit listed in the references) that has been published elsewhere. Students may also submit papers that have been submitted for a grade in a UIC class. The journal also provides an opportunity for all bioengineering students to be involved as editors and reviewers. Thus, working on the publication of the journal will provide students with an overall appreciation of the processes involved in submitting, editing, and disseminating scientific findings. Additionally, through the publication of each issue, the journal serves to expose the authors, reviewers, and readers to current trends in the bioengineering field.

Scope

Submissions can range from original research articles and technical reviews to book or software reviews relevant to bioengineering. Letters to the editor are also welcome. Completed research projects are not necessary for publication. It is expected that some of the articles that appear in the journal will later be expanded into full-length studies and published elsewhere. Publication in the BSJ does not preclude later publication of the results in a copyrighted technical journal.

Bylaw

1. Editorial Board

   The BSJ shall elect one Chief Editor, one Editor-Elect, and one or more Associate Editors during the final week of classes. Editors shall be elected based on a vote of the current editorial board, reviewers, and authors. Editors must have at least one semester of experience participating in the journal, and must display qualities desired of an Editor such as active participation and timely completion of deadlines, and the Chief Editor must have held the position of Editor for at least one semester. When a new Chief Editor is chosen, they shall receive control of the BSJ Google Drive folder. The Editor-Elect shall continue in the position of the editor in the following semester. If the performance of the Editor-Elect is deemed unsatisfactory, including such factors as level of participation and interpersonal skills, the rest of the editorial board may choose a different editor to be Chief Editor the following semester. It is the responsibility of the Chief Editor to keep in regular contact with the Faculty Advisor and Department head about developments in the journal as well as update and maintain the Google Drive folder. Questions and concerns should be brought to the attention of the Faculty Advisor before anyone else. Finished journals and any funds raised should be sent to Jay Lin (jlin13@uic.edu).

2. Meetings

   The BSJ shall have general body meetings, to be held throughout the semester. One meeting must be held within the first two weeks of the semester, and at least once monthly afterwards. Meetings should introduce the journal to interested students and update members on paper statuses. Meeting times are to be finalized during the third week of school between 1:00pm-6:00pm on a day when the highest possible amount of board members can attend.

3. Articles

Papers must follow the BSJ article template, available on Blackboard and the Google Drive folder. Content may include original research, technical reviews, book reviews, or software reviews. Other subjects may be allowed on a case-by-case basis. In the event that a paper authored by more than one student is submitted, names shall be listed in alphabetical order and each student must be involved in the review process. Papers shall be limited to two authors. No member may be the author of more than one paper per publication.

4. Membership

Only bioengineering students may participate in the BSJ. In the event that a student from another major submits a paper, it shall be accepted on a case-by-case basis, depending on the quality of the paper and the number of previously submitted papers. To become a member, either as a reviewer or an author, interested students may email any of the editors, or the BSJ email account (bioejour@uic.edu).

Note: 1) Please use Page Size: 'Letter' not 'A4' 2) Set Margins: 1" for all sides

TITLE OF THE ARTICLE

Author Name
e-mail

Abstract

The title should be 14pt, bold, Times New Roman all capitals. The author name must be in 12pt, Times New Roman, and email in 11pt Italics Times New Roman The abstract should be displayed in a 10pt, italic, Times New Roman font, justified, single column, with an additional left and right indentation of half an inch from the margin. Limit abstract to 300 words.

Keywords: *Template, UIC, Bioengineering, Student, Journal*

1. Introduction

This document represents the format for submissions to the student journal. The two-column format is followed for the body of the article. Text font should be 10pt Times New Roman, justified, single-spaced.

A single empty line should separate paragraphs, the end and beginning of different sections, and must be inserted above and below figures, tables, and equations.

2. Example of Numbered Heading

Each heading must be numbered and be in 12 point, bold, Times New Roman font, with the first letter of all words capitalized except for prepositions and conjunctions.

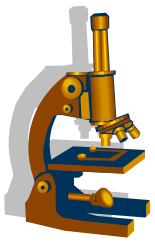

Figure 1. Figure captions are to be below the figure in 9pt Times New Roman, Justified

2.1 Example of Subheading and Table

Subheading must be in 11pt, bold, Times New Roman. Tables should be numbered in the order they appear.

Table 1. This table descriptor is 9pt Times New Roman, Justified

Column 1	Column 2	Column 3	Column 4
Row 1	This	is	Times
Row 2	New	Roman	10pt

3. Equation

Equations should be centered on separate lines with a single space above and below. The equation number should be indicated in parentheses at the rightmost of the last line of the equation.

$$E_{(a-t)} = m*a(s-h) + P_o + A(t)^o * \Sigma(s) \qquad (1)$$

4. Page Limit

Maintain a page limit of 5-10 pages for your entire submission.

List and number all references in 10-pt Times New Roman, single-spaced, at the end of your paper. When referenced in the text, enclose the citation number in square brackets, for example [1]. For multiple references separate using comma(s) [2, 6]. Where appropriate, include the name(s) of editors of referenced books. Arrange all references in alphabetical order of the 'Last Name' as demonstrated in the examples below.

5. References

(Reference format from Annals of Biomedical Engineering)

1. Guccione, J. M., A. D. McCulloch, and L. K. Waldman. Passive material properties of intact ventricular myocardium determined from a cylindrical model. *J. Biomech. Eng. Trans. ASME* 113: 42-55, 1991

2. Rideout, V. C. Mathematical Computer Modeling of Physiological Systems. Prentice Hall, Englewood Cliffs, NJ, 261 p.p., 1991

RICHARD AND LOAN HILL DEPARTMENT OF BIOENGINEERING

COLLEGES OF ENGINEERING AND MEDICINE

UIC